Structure Activity Relationship Study of the XIP Quorum Sensing Pheromone in *Streptococcus mutans* Reveal Inhibitors of the Competence Regulon

Chowdhury Raihan Bikash and Yftah Tal-Gan*

Department of Chemistry, University of Nevada, Reno, 1664 North Virginia Street, Reno, NV 89557

Supporting Information.

* To whom correspondence should be addressed. ytalgan@unr.edu

Additional experimental details

Peptide synthesis

Solid Phase Peptide Synthesis. All the XIP analogs were synthesized using standard Fmoc-based solid-phase peptide synthesis (SPPS) procedures on 4-benzyloxybenzyl alcohol (Wang) resin. Loading of the first amino acid to the Wang resin linker was done by using the symmetrical anhydride procedure as described below.

Loading to Resin. 0.1 g of Wang resin (0.94 mmol/g) was placed in a clean, dry round bottom flask with a minimal amount of DMF to fully cover the resin, and the resin was allowed to swell at room temperature for 30 min. 0.94 mmol (10 equiv. relative to the overall loading of the resin) of Fmoc-protected amino acid were dissolved in dry DCM and placed on an ice bath. A few drops of DMF were added to aid complete dissolution when the amino acid had low solubility in DCM. A solution of 0.47 mmol (5 equiv. relative to the overall loading of the resin) diisopropylcarbodiimide (DIC) in dry DCM was then added dropwise to the amino acid solution. The mixture was stirred for 20 min on an ice bath and the DCM was removed from the mixture using a rotary evaporator. The residue was then dissolved with a minimal amount of DMF and the solution was added to the resin. 0.0094 mmol (0.1 equiv. relative to the overall loading of the resin) of dimethylaminopyridine (DMAP) were dissolved in DMF and the solution was added to the reaction mixture. The mixture was sealed and allowed to stand at room temperature for 2 h with occasional swirling. The resin was washed with DCM, then diethyl ether, followed by overnight drying under vacuum.

Loading Test. Two small samples of the amino acid-loaded resin (approximately 5 mg each) were weighed and mixed with 3 mL of fresh 20% piperidine in DMF solution. This solution was stirred on a shaker for 2 h. The absorbance (290 nm) of the supernatants of the two piperidine-resin mixtures was measured by using a UV-Vis spectrophotometer to estimate the level of Fmoc removal, which correlates to first residue attachment. The first residue attachment was estimated from the following equations:

Equation 1 $$A\ (mmol/g) = B \times 1000/[1000 + (B\ \times (M - X))]$$

A is the theoretical substitution (mmol/g), B is the substitution of starting resin (mmol/g), and M is the molecular weight of target peptide with all protecting groups. X is 18 for hydroxymethyl-based resin.

Equation 2 $$B\ (mmol/g) = (Abs_{sample}\ \times\ N)/(mg\ of\ sample\ \times 1.75)$$

B is the experimental first residue attachment and the equation is based on $\varepsilon = 5253\ M^{-1}\ cm^{-1}$. N is the fold of dilution of the supernatant. $\frac{B}{A} \times 100\%$ is the percent yield of the loading. If the average of the percent yield of the two samples was greater than 70%, resin loading was deemed successful and the resin would be used for the synthesis of XIP analogs.

Synthesis. XIP and XIP analogs were synthesized with the Liberty1 automated peptide synthesizer (CEM Corporation) (Coupling, 75 °C / 5 min and Deprotection, 90 °C / 90 sec). For the deprotection, 20% piperidine in DMF was used and for the coupling, Fmoc-protected amino acids (5 equiv.), 2-(1H-benzotriazol-1-yl)-1,1,3,3-tetramethyluronium hexafluorophosphate (HBTU; 5 equiv.) and diisopropylethylamine (DIPEA; 10 equiv.) were used.

Cleavage. Upon completion of peptide synthesis, the resin was washed with diethyl ether (2 mL) and dried under nitrogen stream for 3 min before it was transferred into a 15 mL falcon tube. The peptide was cleaved from the resin, along with all of the protecting groups, by mixing the resin with 3 mL cleavage cocktail of 95% trifluoroacetic acid (TFA), 2.5% triisopropylsilane (TIPS), and 2.5% 18 MΩ water for 3 h with agitation. The resulting cleavage product solution was separated from the resin by filtration and the filtrate was transferred into a new 50 mL falcon tube. A cooled solution of diethyl ether:hexane (1:1, 45 mL, 0 °C) was added to the filtrate, and the peptide was allowed to precipitate for 10 min in a freezer at -20 °C. The mixture was centrifuged for 5 min at 3000 RPM and the supernatant was removed to yield crude peptide that was dissolved in 10 mL acetonitrile (ACN):water (1:1) and lyophilized before HPLC purification.

Peptide Purification. Crude peptides were purified with RP-HPLC. A semipreparative Phenomenex Kinetex C18 column (5 μm, 10 mm × 250 mm, 110 Å) was used for preparative RP-HPLC work, while an analytical Phenomenex Kinetex C18 column (5 μm, 4.6 mm × 250 mm, 110 Å) was used for analytical RP-HPLC work. Standard RP-HPLC conditions were as follows: flow rates = 5 mL min^{-1} for semipreparative separations and 1 mL min^{-1} for analytical separations; mobile phase A = 18 MΩ water + 0.1% TFA; mobile phase B = ACN + 0.1% TFA. Purities were determined by integration of peaks with UV detection at 220 nm. Preparative HPLC methods were used to separate the crude peptide mixture to different chemical components using a linear gradient (first prep 5% B → 45% B over 40 min and second prep 20% B → 30% B over 30 min), except for the di- and tri-peptide analogs. A different linear gradient (5% B → 25% B over 40 min) was used for prep purifications of the di- and tri-peptide analogs (a single prep run was sufficient to purify the di- and tri-peptides to >95% purity). Then, an analytical HPLC method was used to quantify the purity of the desired product using a linear gradient (5% B → 95% B over 27 min). Only peptide fractions that were purified to homogeneity (>95%) were used for the biological assays. Exact Mass was used to validate the presence of synthesized peptides. The observed mass-to-charge (m/z) ratio of the peptide was compared to the expected m/z ratio for each peptide.

Biological assays

Bacterial Growth Conditions for CDM. Bacteria from freezer stocks were streaked onto a THY agar plate containing 5 μg/mL erythromycin (*S. mutans* SMCOM2) or 250 μg/mL kanamycin (*S. mutans* SAB249). The plate was incubated for 22-24 h in a CO_2 incubator (37 °C with 5% CO_2). A fresh single colony was transferred to 5 mL of BHI broth supplemented with a final concentration of 5 μg/mL erythromycin (*S. mutans* SMCOM2) or 250 μg/mL kanamycin (*S. mutans* SAB249) and the culture was incubated in a CO_2 incubator overnight (15 h). Overnight culture was then diluted 1:25 with BHI, and the resulting solution was incubated in a CO_2 incubator for 2.5 h, until the bacteria reached early exponential stage (0.15−0.16 OD 600_{nm}) as determined by using a plate reader. After that, cells were centrifuged at 5000 rpm for 10 min and BHI medium was discarded. Then, cells were washed and centrifuged (5 min at 5000 rpm) two times with 5 mL sterile PBS buffer. PBS buffer was discarded and the cells were resuspended in CDM media and vortexed for 10 sec followed by 25 min incubation in a shaking incubator at 37 °C to allow the bacteria cells to adapt to the new media environment before they were used in the different CDM assays.

Beta-Galactosidase Activation Assays in CDM. The ability of synthetic XIP analogs to activate the expression of *comX* was determined using the *S. mutans* SMCOM2 reporter strain in CDM (*S. mutans* SAB249 reporter strain was only used to check the inhibitory activity of the lead inhibitor in presence of CSP and XIP). An initial activation screening was performed at a high concentration (100 μM) for all XIP analogs. A total of 2 μL of 10 mM solution of XIP analogs in dimethyl sulfoxide (DMSO) was added in triplicate to a clear 96-well microtiter plate. This concentration was chosen to afford full activation of the QS circuit, as determined from the dose-dependent curve created for the native XIP. A total of 2 μL of DMSO was added in triplicate and served as the negative control, while 2 μL of native XIP in DMSO was added in triplicate and served as the positive control. Then, 198 μL of bacterial culture in CDM was added to each well containing XIP and analogs. The plate was incubated at 37 °C for 1 h, and the OD 600_{nm} was measured. In order to measure the beta-galactosidase activity in the culture, the cells were lysed by incubating the culture for 30 min at 37 °C with 20 μL of 0.1% Triton X-100. In a new plate, 100 μL of Z-buffer solution (60.2 mM Na_2HPO_4, 45.8 mM NaH_2PO_4, 10 mM KCl, and 1.0 mM $MgSO_4$ in 18 MΩ H_2O; pH was adjusted to 7.0, and the buffer was sterilized before use) containing 2-nitrophenyl-beta-D-galactopyranoside (ONPG) at a final concentration of 0.4 mg mL^{-1} was added, followed by 100 μL of lysate, and the plate was incubated for 30 min at 37 °C. The reaction was stopped by adding 50 μL of 1 M sodium carbonate solution, and the OD 420_{nm} and OD 550_{nm} were measured using a plate reader. The final results were reported as percent activation, which is the ratio between the Miller units of the analog and of the positive control. For calculation of Miller units, please see data analysis section below. Analogs that exhibited high activity in the initial screening (>50% activation compared to the native signal; see **Figures**

S-1 and S-2) were further evaluated using a dose-dependent assay in which peptide stock solutions were diluted with DMSO in serial dilutions (either 1:2, 1:3, or 1:5) and assayed as described above. GraphPad Prism 5 was used to calculate the EC_{50} values, which are the concentration of a drug that gives half-maximal response.

Beta-Galactosidase Inhibition Assays in CDM. Analogs that exhibited low *comX* activation in the initial screening (see **Figure S-1 and S-2**) were evaluated for competitive inhibition (see **Figure S-3**). The ability of synthetic XIP analogs to inhibit the expression of *comX* by outcompeting XIP for the ComR binding site was evaluated using the same assay conditions as described above, except that in the initial inhibition screening, the native XIP was added to every well in a set concentration (2000 nM final concentration) that was chosen to afford full activation of the QS circuit, as determined from the dose-dependent curve created for the native XIP. A total of 2 μL of 200 μM solution of native XIP and 2 μL of 10 mM solution of XIP analogs were added to the same well in triplicate in a clear 96-well microtiter plate. A total of 2 μL of native XIP and 2 μL of DMSO were added to the same well in triplicate and served as the positive control. A total of 4 μL of DMSO was added in triplicate and served as the negative control. Then, 196 μL of bacterial culture in CDM was added to the wells, and the plate was incubated at 37 °C for 1 h. The procedure for lysis, incubation with ONPG, and all the measurements were as described in the activation assay.

Bacterial Growth Conditions for complex media (THY). A fresh single colony was transferred to 5 mL of THY broth supplemented with a final concentration of 250 μg/mL kanamycin (*S. mutans* SAB249) or 5 μg/mL erythromycin (*S. mutans* SMCOM2) and the culture was incubated in a CO_2 incubator overnight (15 h). Overnight culture was then diluted 1:25 with THY, and the resulting solution was incubated in a CO_2 incubator for 2 h, until the bacteria reached early exponential stage (0.17−0.19) as determined by using a plate reader.

HPLC traces for XIP analogs

XIP (P1)

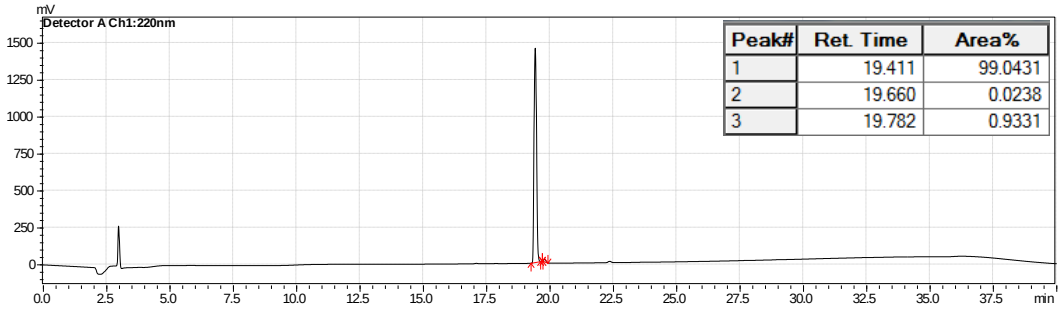

Peak#	Ret. Time	Area%
1	19.411	99.0431
2	19.660	0.0238
3	19.782	0.9331

XIP-G1A (P2)

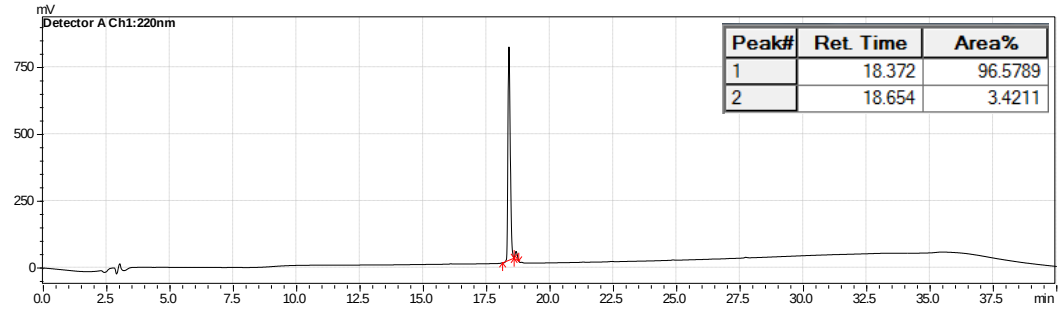

Peak#	Ret. Time	Area%
1	18.372	96.5789
2	18.654	3.4211

XIP-L2A (P3)

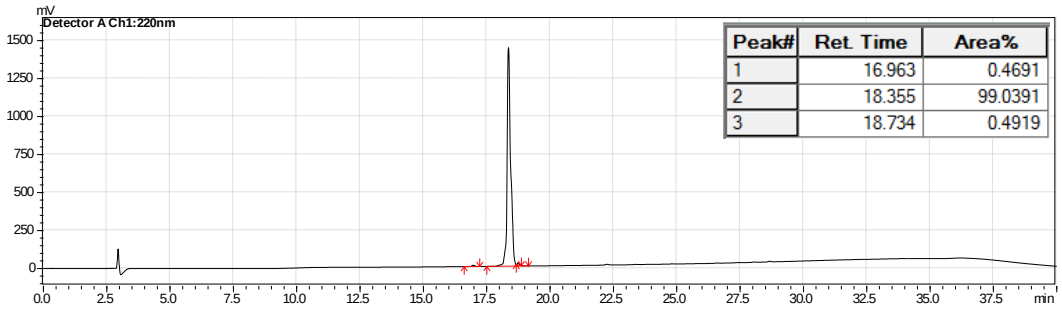

Peak#	Ret. Time	Area%
1	16.963	0.4691
2	18.355	99.0391
3	18.734	0.4919

XIP-D3A (P4)

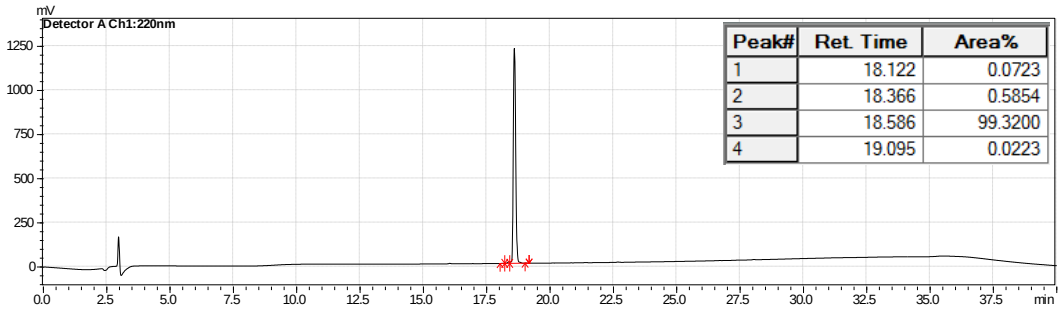

Peak#	Ret. Time	Area%
1	18.122	0.0723
2	18.366	0.5854
3	18.586	99.3200
4	19.095	0.0223

XIP-W4A (P5)

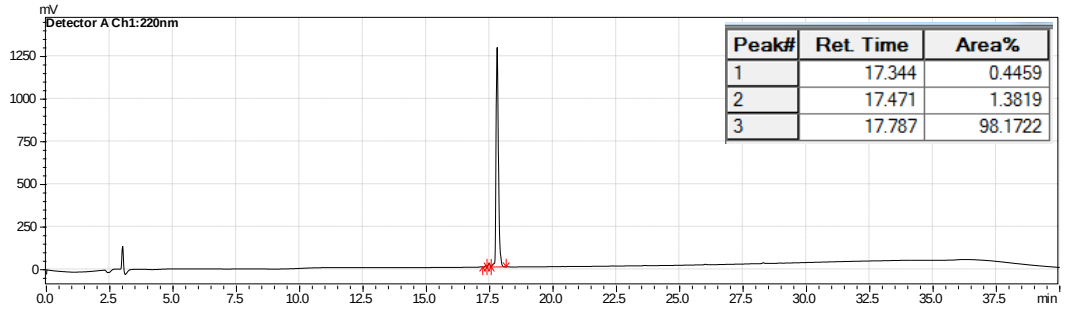

Peak#	Ret. Time	Area%
1	17.344	0.4459
2	17.471	1.3819
3	17.787	98.1722

XIP-W5A (P6)

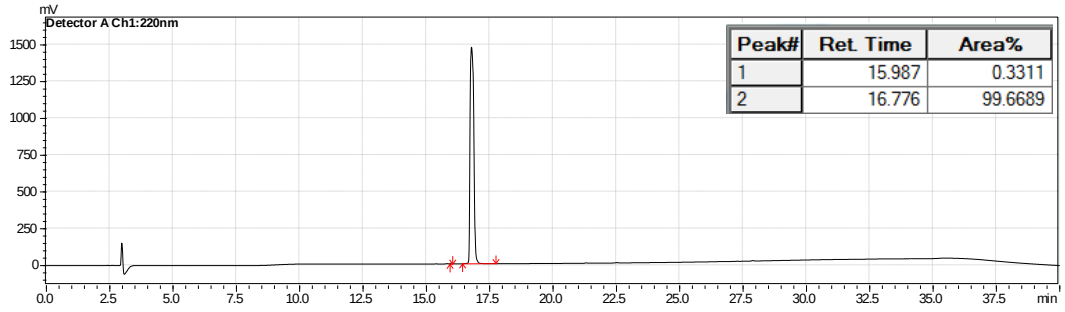

Peak#	Ret. Time	Area%
1	15.987	0.3311
2	16.776	99.6689

XIP-S6A (P7)

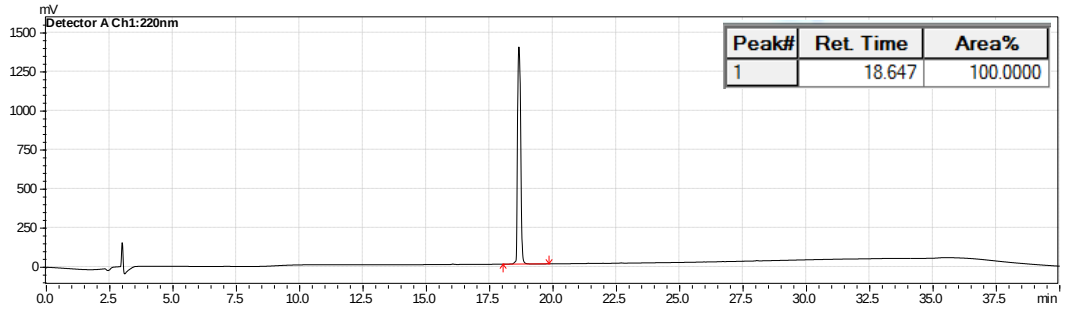

Peak#	Ret. Time	Area%
1	18.647	100.0000

XIP-L7A (P8)

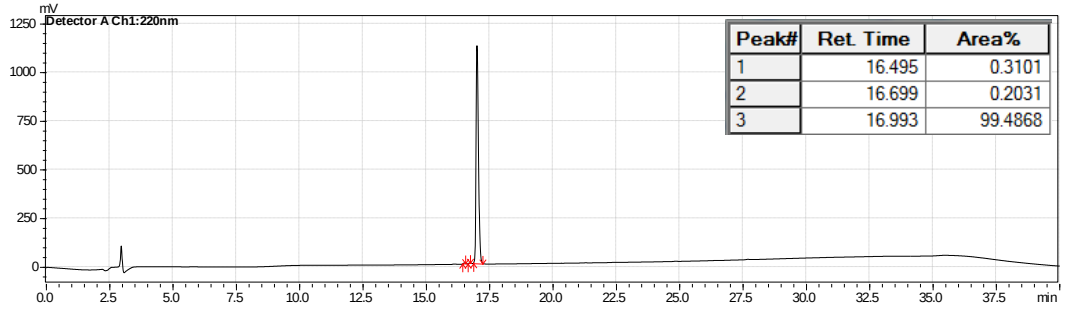

Peak#	Ret. Time	Area%
1	16.495	0.3101
2	16.699	0.2031
3	16.993	99.4868

XIP-l2 (P9)

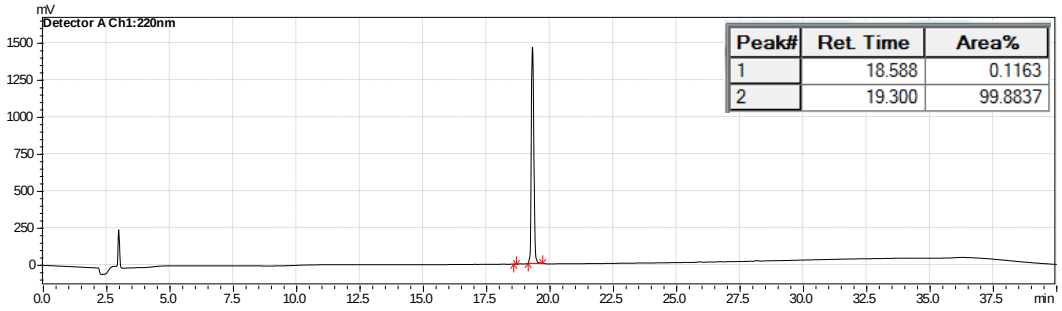

Peak#	Ret. Time	Area%
1	18.588	0.1163
2	19.300	99.8837

XIP-d3 (P10)

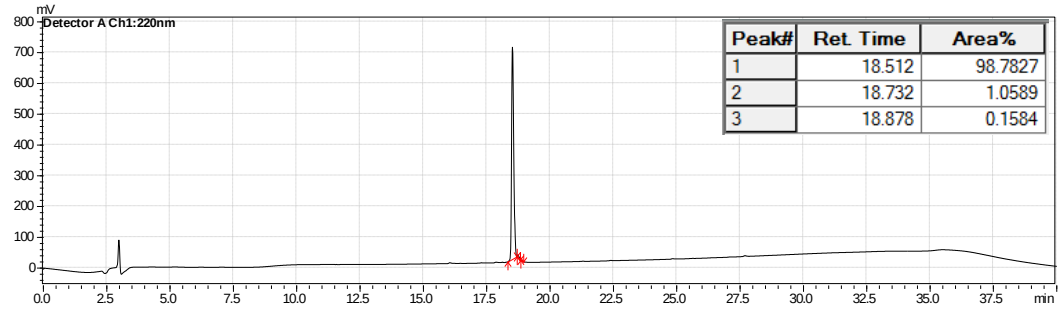

Peak#	Ret. Time	Area%
1	18.512	98.7827
2	18.732	1.0589
3	18.878	0.1584

XIP-w4 (P11)

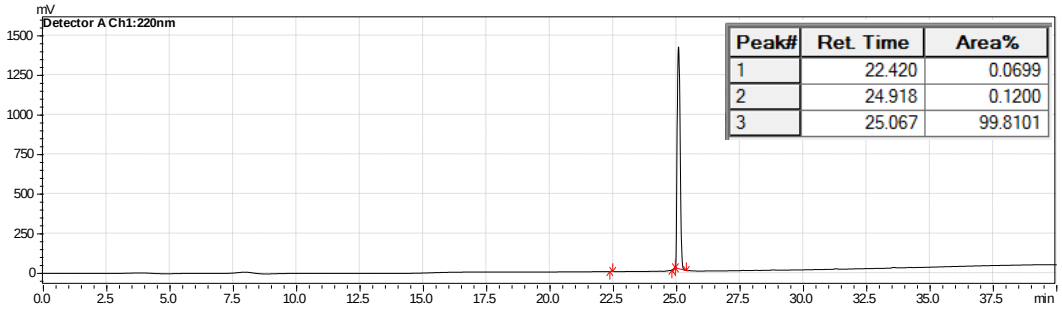

Peak#	Ret. Time	Area%
1	22.420	0.0699
2	24.918	0.1200
3	25.067	99.8101

XIP-w5 (P12)

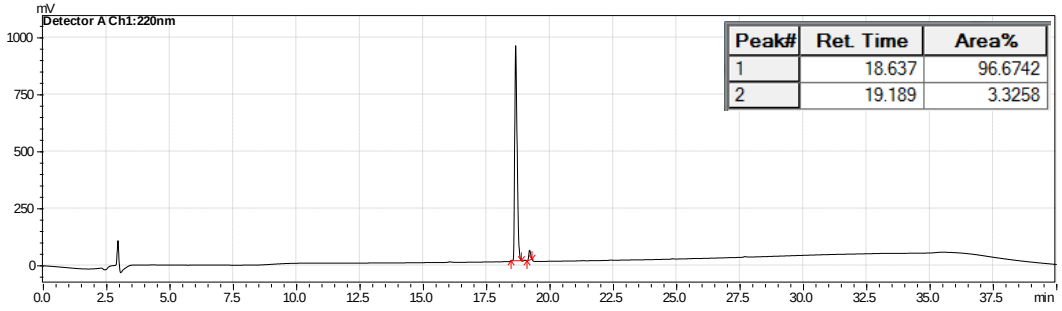

Peak#	Ret. Time	Area%
1	18.637	96.6742
2	19.189	3.3258

XIP-s6 (P13)

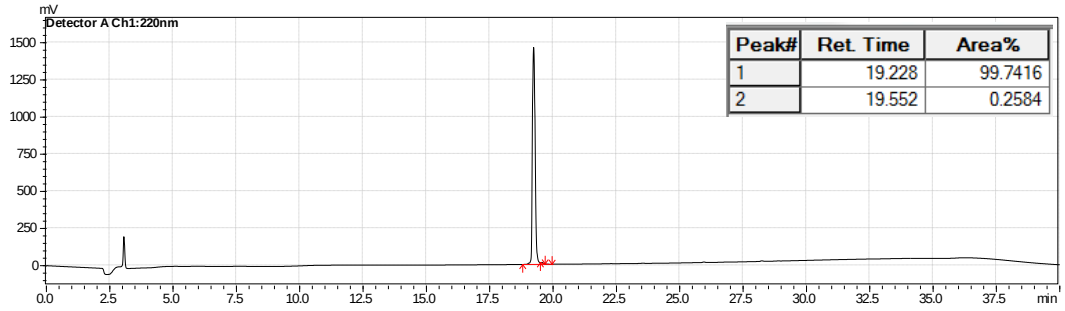

Peak#	Ret. Time	Area%
1	19.228	99.7416
2	19.552	0.2584

XIP-l7 (P14)

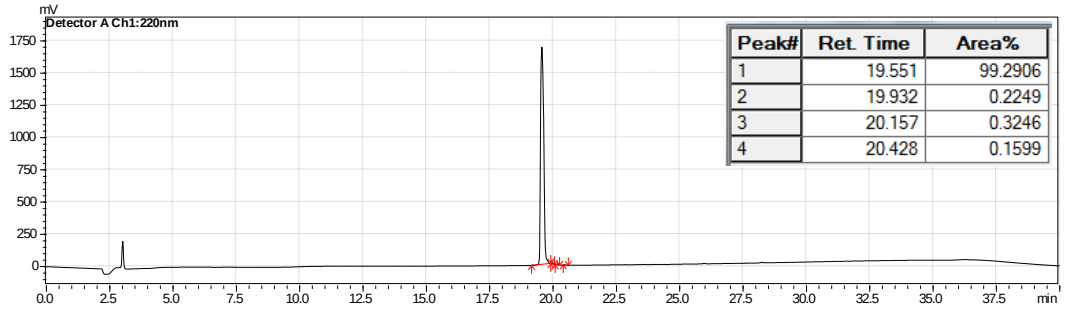

Peak#	Ret. Time	Area%
1	19.551	99.2906
2	19.932	0.2249
3	20.157	0.3246
4	20.428	0.1599

XIP-L2I (P15)

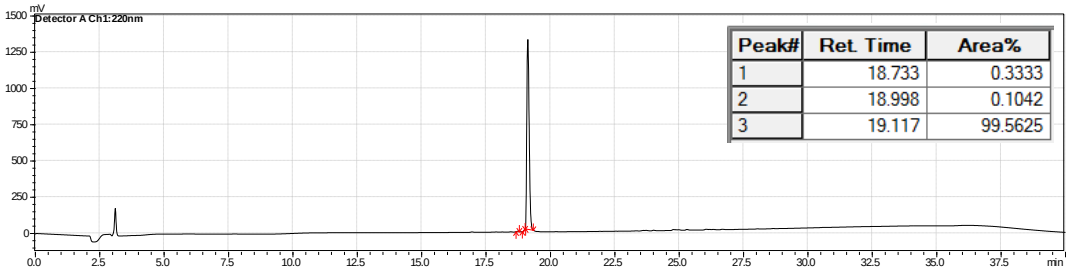

Peak#	Ret. Time	Area%
1	18.733	0.3333
2	18.998	0.1042
3	19.117	99.5625

XIP-L2V (P16)

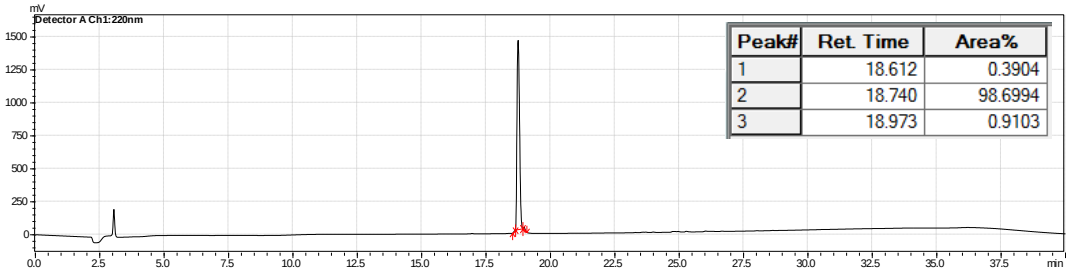

Peak#	Ret. Time	Area%
1	18.612	0.3904
2	18.740	98.6994
3	18.973	0.9103

XIP-L2NL (P17)

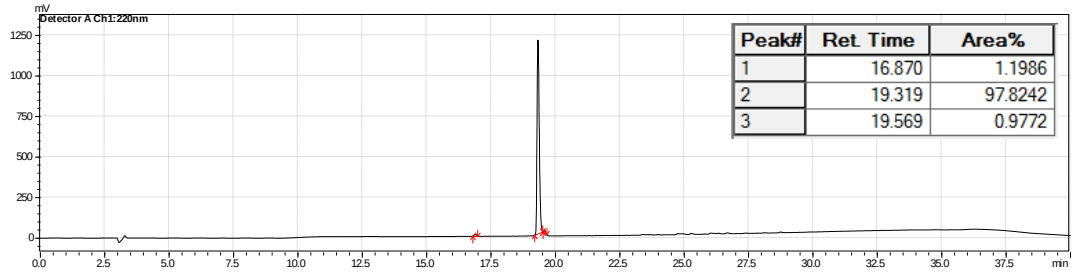

Peak#	Ret. Time	Area%
1	16.870	1.1986
2	19.319	97.8242
3	19.569	0.9772

XIP-L2NV (P18)

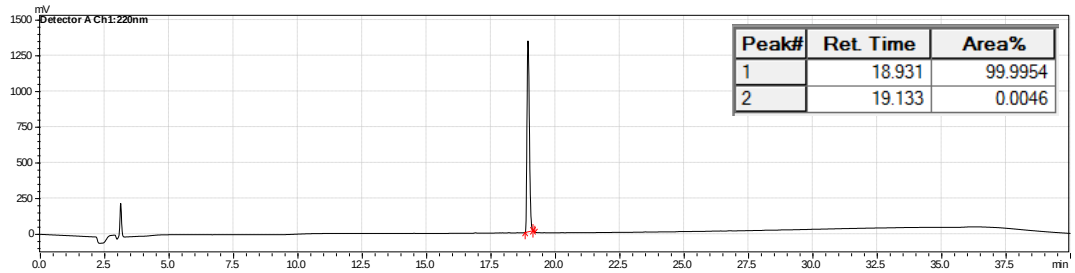

Peak#	Ret. Time	Area%
1	18.931	99.9954
2	19.133	0.0046

XIP-W4F (P19)

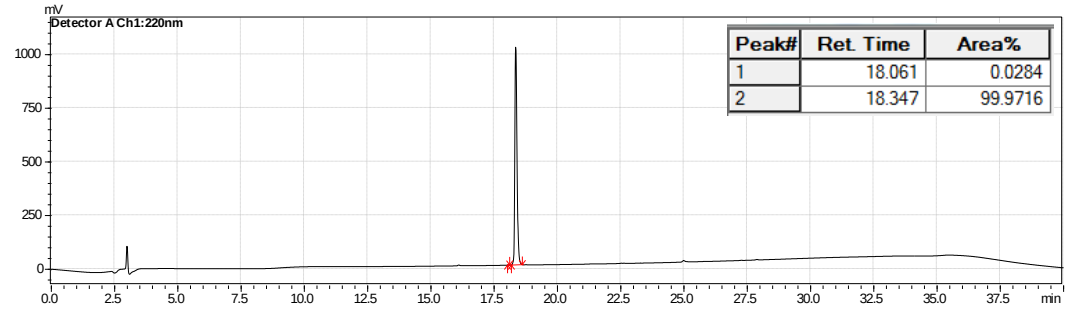

Peak#	Ret. Time	Area%
1	18.061	0.0284
2	18.347	99.9716

XIP-W4Y (P20)

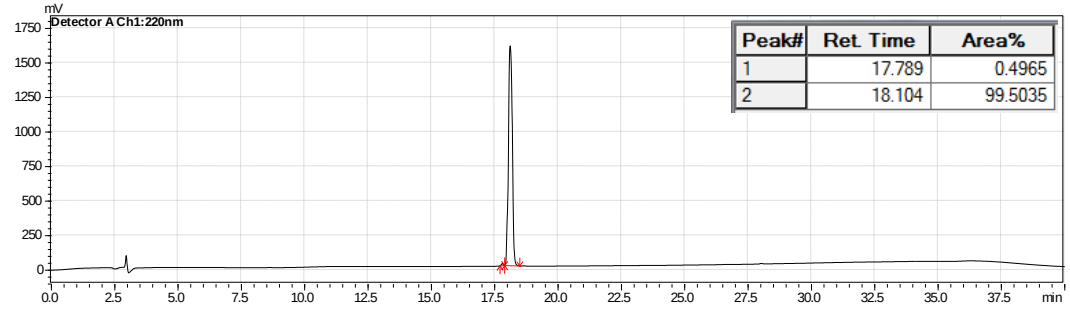

Peak#	Ret. Time	Area%
1	17.789	0.4965
2	18.104	99.5035

XIP-W4Cha (P21)

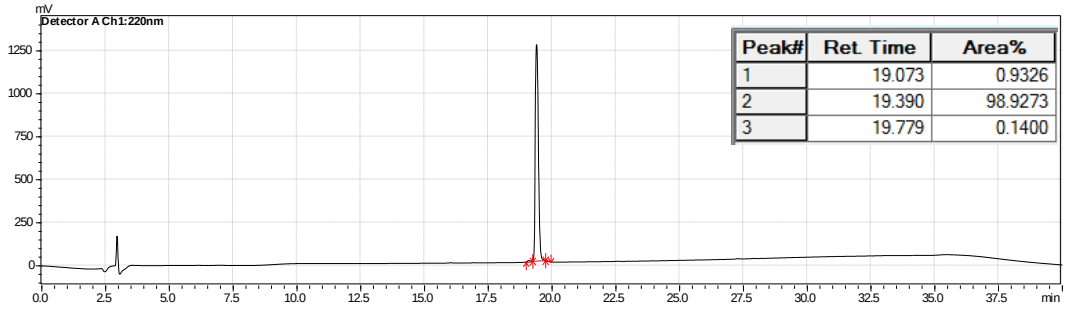

Peak#	Ret. Time	Area%
1	19.073	0.9326
2	19.390	98.9273
3	19.779	0.1400

XIP-W5F (P22)

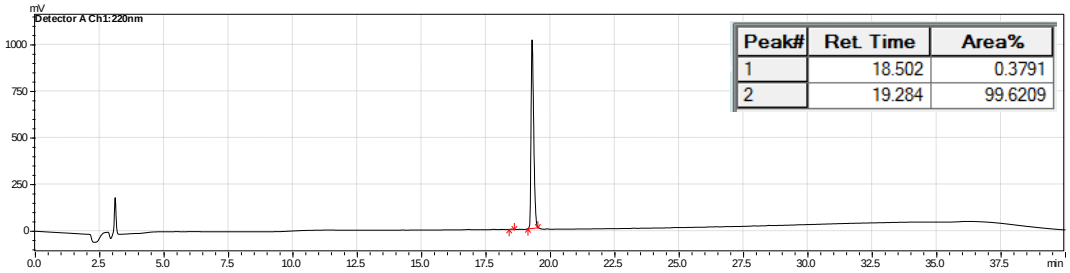

Peak#	Ret. Time	Area%
1	18.502	0.3791
2	19.284	99.6209

XIP-W5Y (P23)

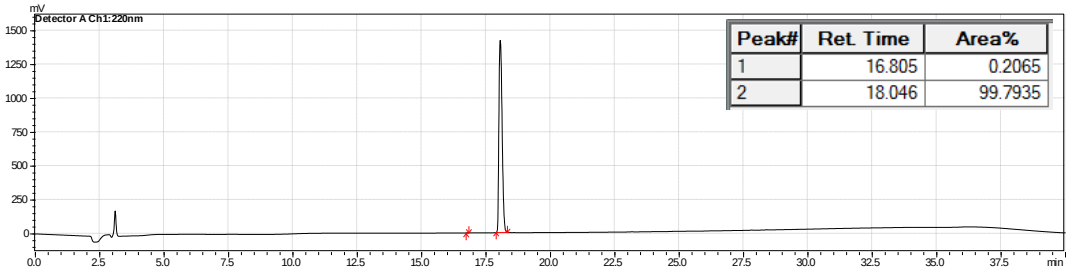

Peak#	Ret. Time	Area%
1	16.805	0.2065
2	18.046	99.7935

XIP-W5Cha (P24)

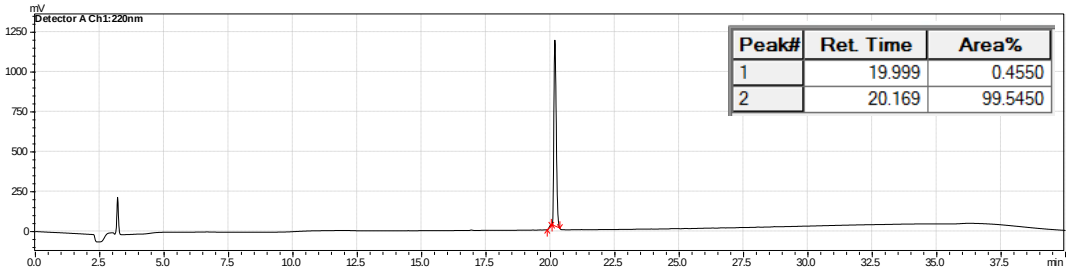

Peak#	Ret. Time	Area%
1	19.999	0.4550
2	20.169	99.5450

XIP-L7I (P25)

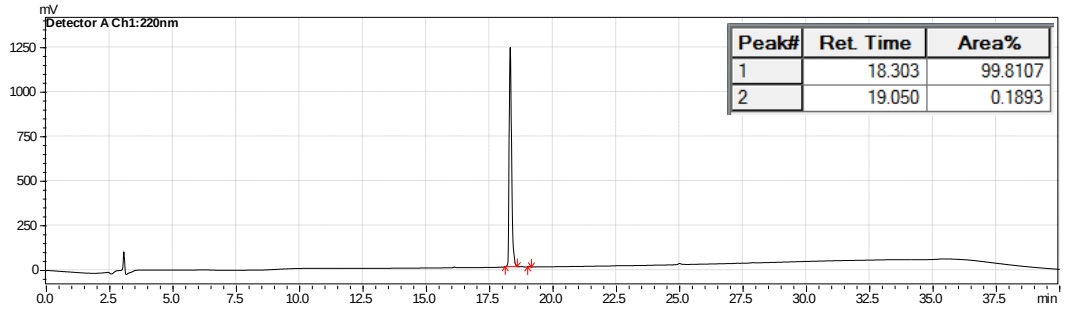

Peak#	Ret. Time	Area%
1	18.303	99.8107
2	19.050	0.1893

XIP-L7V (P26)

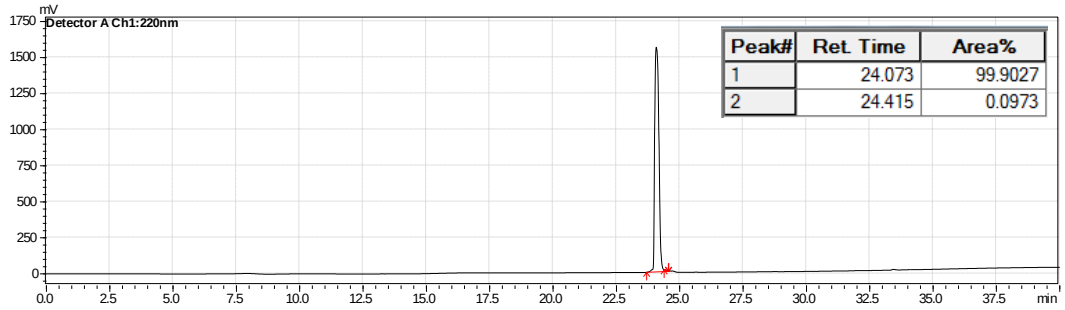

Peak#	Ret. Time	Area%
1	24.073	99.9027
2	24.415	0.0973

XIP-L7NL (P27)

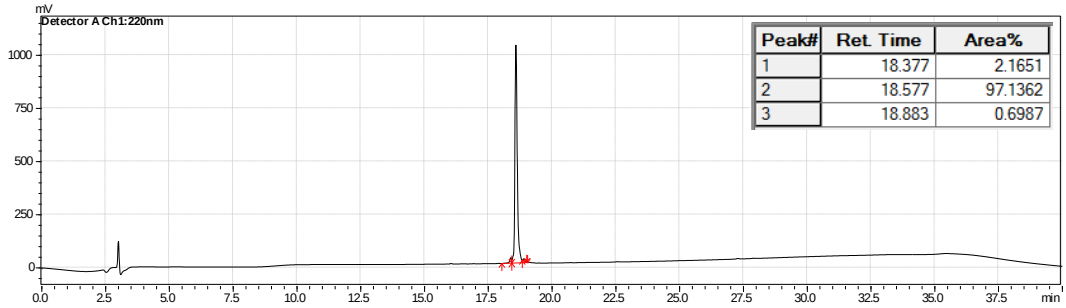

Peak#	Ret. Time	Area%
1	18.377	2.1651
2	18.577	97.1362
3	18.883	0.6987

XIP-L7NV (P28)

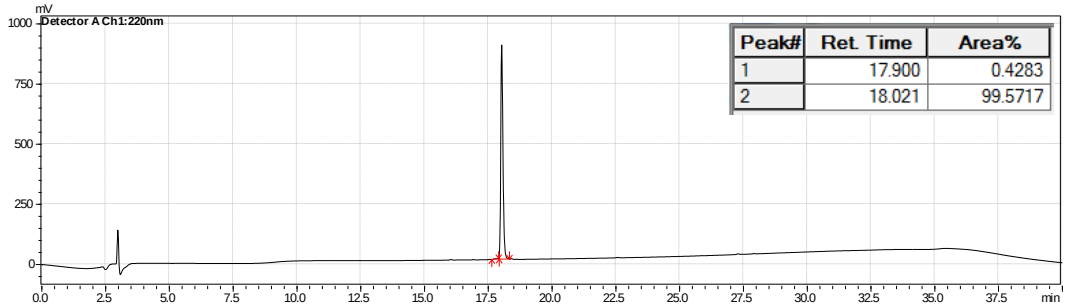

Peak#	Ret. Time	Area%
1	17.900	0.4283
2	18.021	99.5717

XIP-W4AL7A (P29)

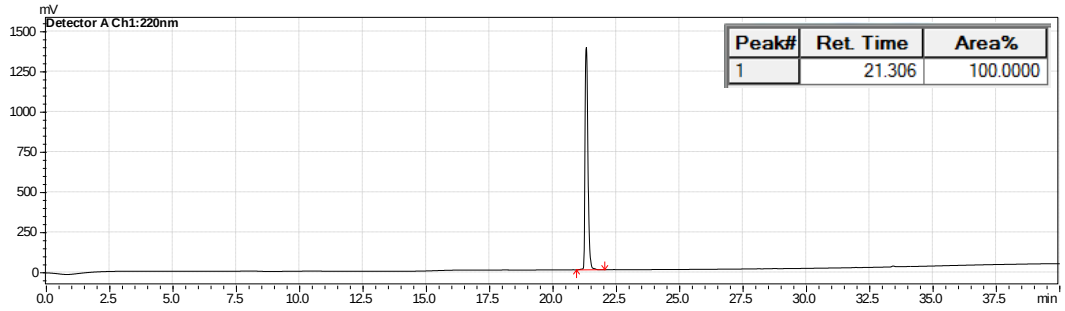

Peak#	Ret. Time	Area%
1	21.306	100.0000

XIP-G1AD3AS6A (P30)

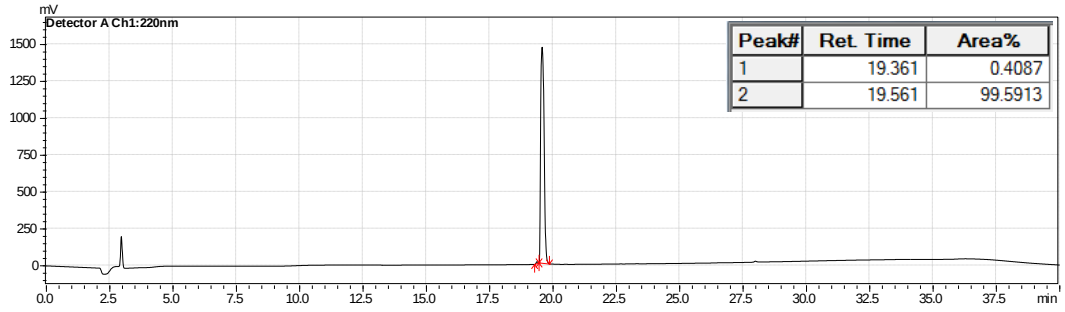

Peak#	Ret. Time	Area%
1	19.361	0.4087
2	19.561	99.5913

XIP-G1AD3AW4YS6A (P31)

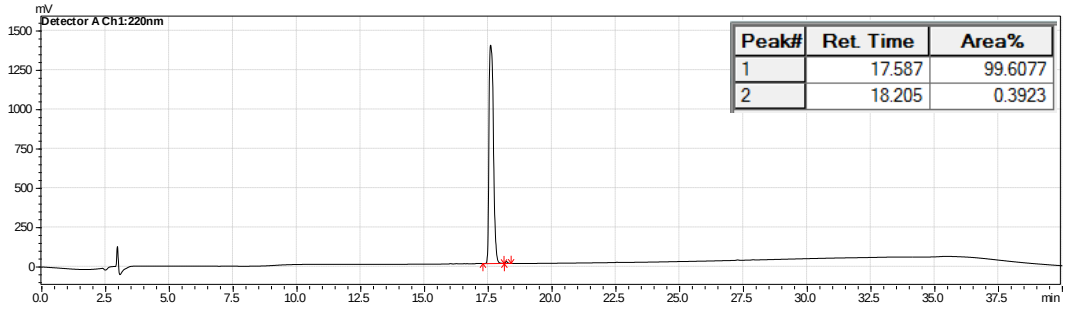

Peak#	Ret. Time	Area%
1	17.587	99.6077
2	18.205	0.3923

XIP-G1AD3AW4AS6A (P32)

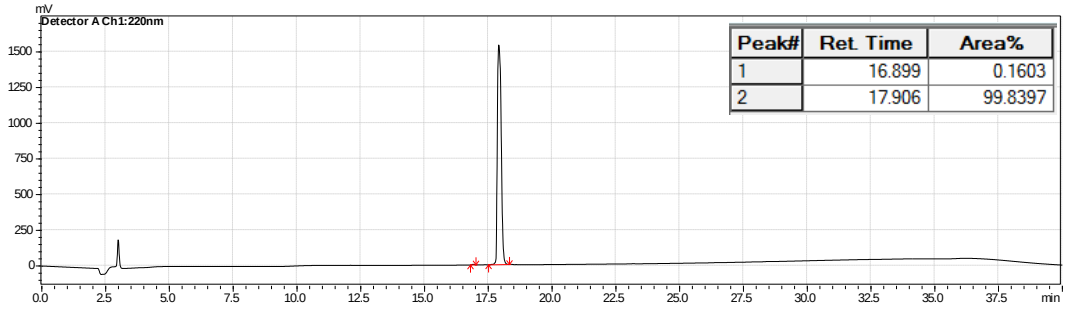

Peak#	Ret. Time	Area%
1	16.899	0.1603
2	17.906	99.8397

XIP-G1AD3AS6AL7A (P33)

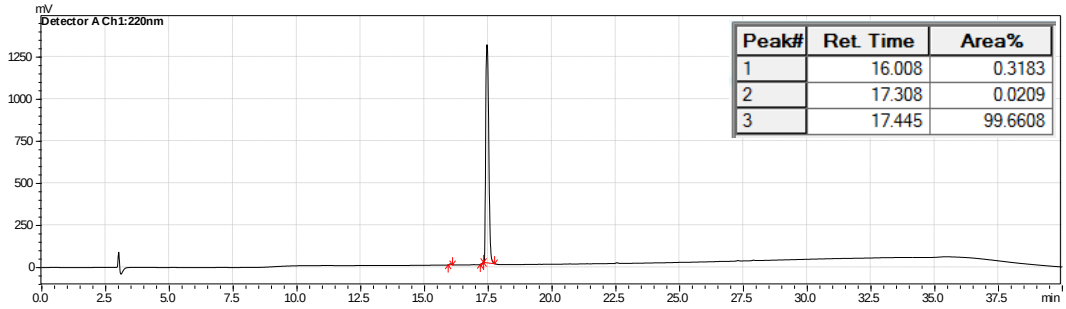

Peak#	Ret. Time	Area%
1	16.008	0.3183
2	17.308	0.0209
3	17.445	99.6608

XIP-G1AD3AW4AS6AL7A (P34)

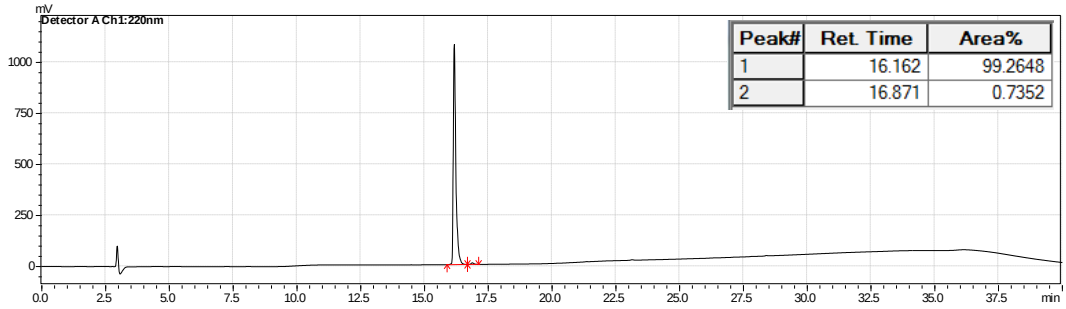

Peak#	Ret. Time	Area%
1	16.162	99.2648
2	16.871	0.7352

XIP-des-G1 (P35)

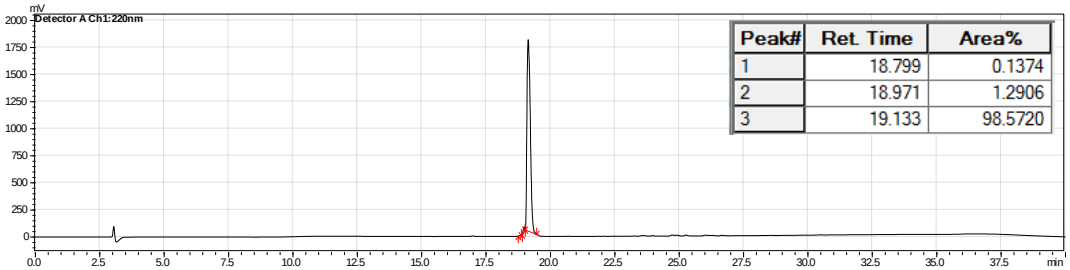

Peak#	Ret. Time	Area%
1	18.799	0.1374
2	18.971	1.2906
3	19.133	98.5720

XIP-des-G1L2 (P36)

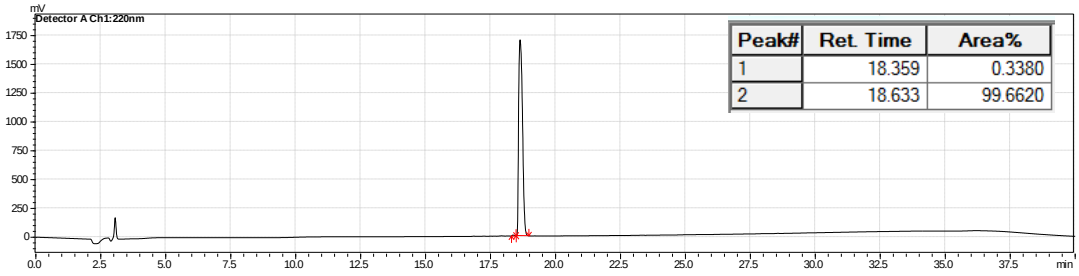

Peak#	Ret. Time	Area%
1	18.359	0.3380
2	18.633	99.6620

XIP-des-G1L2D3 (P37)

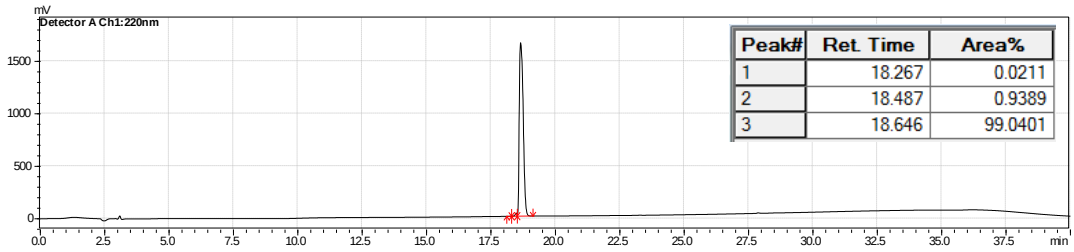

Peak#	Ret. Time	Area%
1	18.267	0.0211
2	18.487	0.9389
3	18.646	99.0401

XIP-des-G1L2D3W4 (P38)

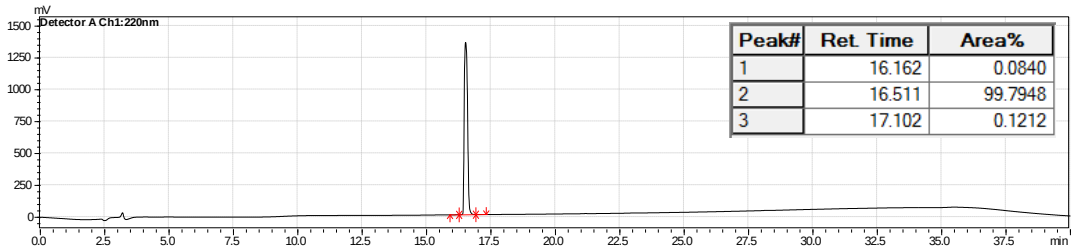

Peak#	Ret. Time	Area%
1	16.162	0.0840
2	16.511	99.7948
3	17.102	0.1212

XIP-Des-G1L2D3W4W5 (P39)

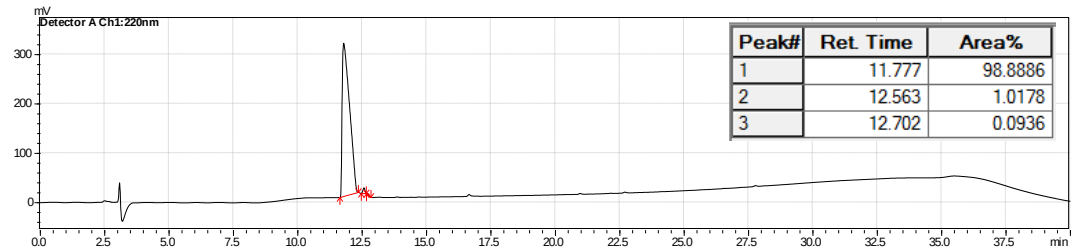

Peak#	Ret. Time	Area%
1	11.777	98.8886
2	12.563	1.0178
3	12.702	0.0936

XIP-des-L7 (P40)

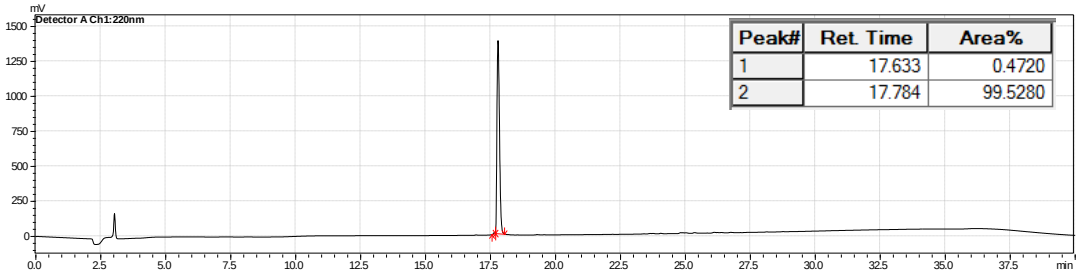

Peak#	Ret. Time	Area%
1	17.633	0.4720
2	17.784	99.5280

XIP-des-S6L7 (P41)

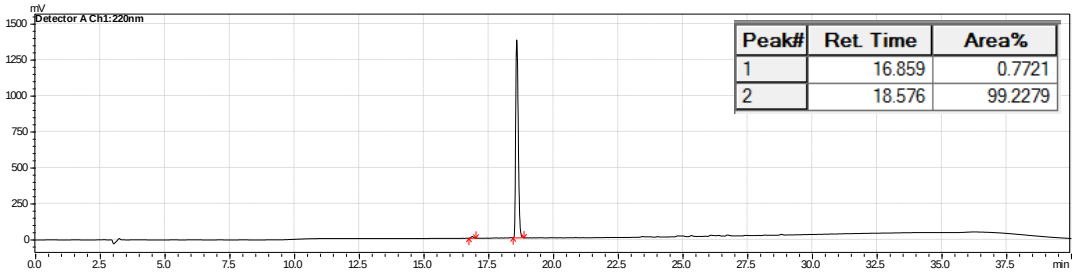

Peak#	Ret. Time	Area%
1	16.859	0.7721
2	18.576	99.2279

XIP-des-W5S6L7 (P42)

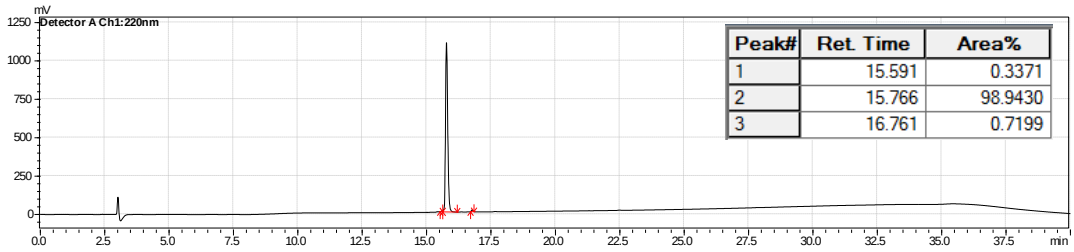

Peak#	Ret. Time	Area%
1	15.591	0.3371
2	15.766	98.9430
3	16.761	0.7199

XIP-Des-W4W5S6L7 (P43)

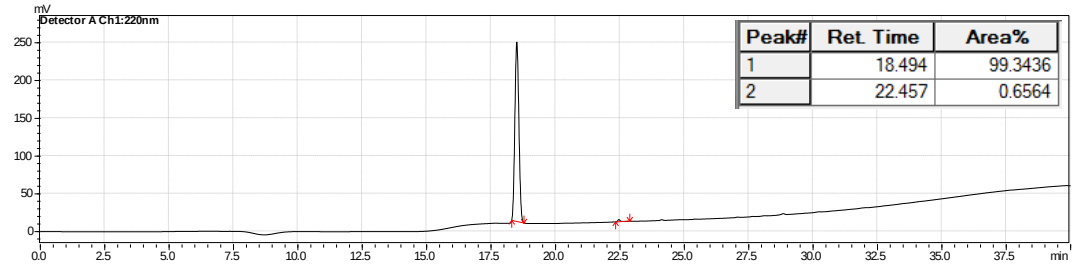

Peak#	Ret. Time	Area%
1	18.494	99.3436
2	22.457	0.6564

XIP-Des-G1L2D3L7 (P44)

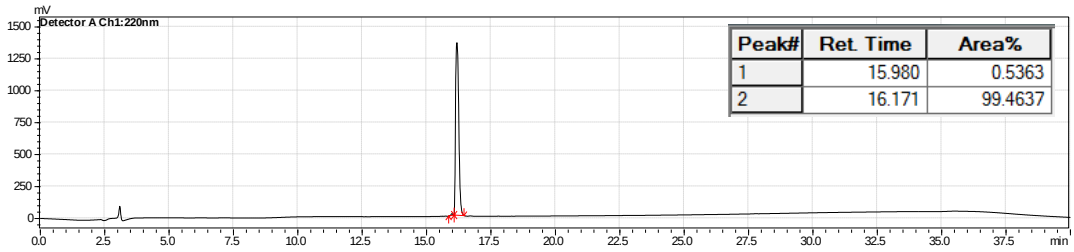

Peak#	Ret. Time	Area%
1	15.980	0.5363
2	16.171	99.4637

XIP-Des-G1L2D3W4L7 (P45)

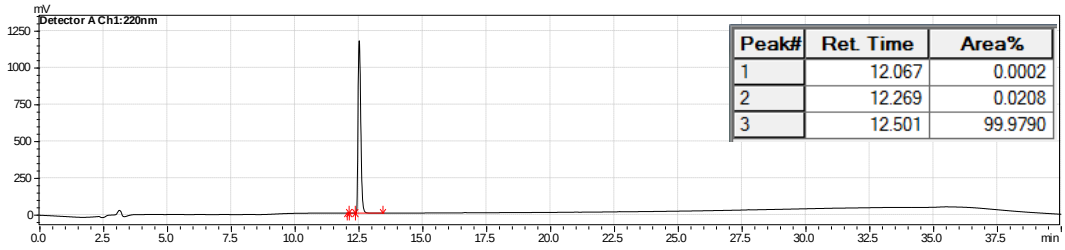

Peak#	Ret. Time	Area%
1	12.067	0.0002
2	12.269	0.0208
3	12.501	99.9790

XIP-Des-G1L2D3S6L7 (P46)

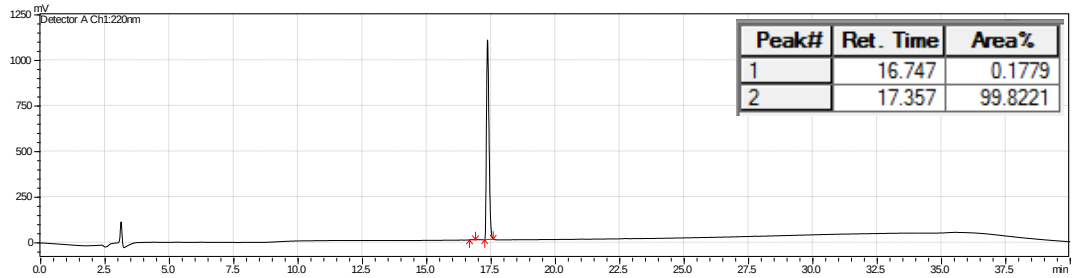

Peak#	Ret. Time	Area%
1	16.747	0.1779
2	17.357	99.8221

MS and HPLC data for XIP analogs

Table S-1. MS and HPLC data for XIP analogs.

Compound Name	Sequence	Calc. EM MH^{1+}	Obs. EM MH^{1+}	Purity (%)
XIP (P1)	GLDWWSL	876.4250	876.4290	>99
XIP-G1A (P2)	ALDWWSL	890.4407	890.4381	>96
XIP-L2A (P3)	GADWWSL	834.3781	834.3740	>99
XIP-D3A (P4)	GLAWWSL	832.4352	832.4326	>99
XIP-W4A (P5)	GLDAWSL	761.3828	761.3817	>98
XIP-W5A (P6)	GLDWASL	761.3828	761.3828	>99
XIP-S6A (P7)	GLDWWAL	860.4301	860.4294	>99
XIP-L7A (P8)	GLDWWSA	834.3781	834.3756	>99
XIP-l2 (P9)	GlDWWSL	876.4250	876.4232	>99
XIP-d3 (P10)	GLdWWSL	876.4250	876.4247	>98
XIP-w4 (P11)	GLDwWSL	876.4250	876.4238	>99
XIP-w5 (P12)	GLDWwSL	876.4250	876.4246	>96
XIP-s6 (P13)	GLDWWsL	876.4250	876.4211	>99
XIP-l7 (P14)	GLDWWSl	876.4250	876.4210	>99
XIP-L2I (P15)	GIDWWSL	876.4250	876.4217	>99
XIP-L2V (P16)	GVDWWSL	862.4094	862.4103	>98
XIP-L2NL (P17)	GnLDWWSL	876.4250	876.4269	>97
XIP-L2NV (P18)	GnVDWWSL	862.4094	862.4112	>99
XIP-W4F (P19)	GLDFWSL	837.4141	837.4156	>99
XIP-W4Y (P20)	GLDWYSL	853.4090	853.4118	>99
XIP-W4Cha (P21)	GLDChaWSL	843.4611	843.4621	>98
XIP-W5F (P22)	GLDWFSL	837.4141	837.4130	>99
XIP-W5Y (P23)	GLDWYSL	853.4090	853.4071	>99
XIP-W5Cha (P24)	GLDWChaSL	843.4611	843.4589	>99
XIP-L7I (P25)	GLDWWSI	876.4250	876.4234	>99
XIP-L7V (P26)	GLDWWSV	862.4094	862.4072	>99
XIP-L7NL (P27)	GLDWWSnL	876.4250	876.4256	>97
XIP-L7NV (P28)	GLDWWSnV	862.4094	862.4097	>99
XIP-W4AL7A (P29)	GLDAWSA	830.4559	830.4537	>99
XIP-G1AD3AS6A (P30)	ALAWWAL	719.3359	719.3374	>99
XIP-G1AD3AW4YS6A (P31)	ALAYWAL	807.4400	807.4418	>99
XIP-G1AD3AW4AS6A (P32)	ALAAWAL	715.4137	715.4154	>99
XIP-G1AD3AS6AL7A (P33)	ALAWWAA	788.4090	788.4100	>99
XIP-G1AD3AW4AS6AL7A (P34)	ALAAWAA	673.3668	673.3678	>99

EM = Exact Mass.

Table S-2. MS and HPLC data for XIP analogs.

Compound Name	Sequence	Calc. EM MH^{1+}	Obs. EM MH^{1+}	Purity (%)
XIP	GLDWWSL	876.4250	876.4290	>99
XIP-des-G1 (P35)	LDWWSL	819.4036	819.4029	>98
XIP-des-G1L2 (P36)	DWWSL	706.3195	706.3184	>99
XIP-des-G1L2D3 (P37)	WWSL	591.2926	591.2908	>99
XIP-des-G1L2D3W4 (P38)	WSL	405.2132	405.2149	>99
XIP-des-G1L2D3W4W5 (P39)	SL	241.1159(+Na)	241.1156	>98
XIP-des-L7 (P40)	GLDWWS	763.3410	763.3391	>99
XIP-des-S6L7 (P41)	GLDWW	676.3089	676.3070	>99
XIP-des-W5S6L7 (P42)	GLDW	490.2296	490.2281	>98
XIP-des-W4W5S6L7 (P43)	GLD	326.1323(+Na)	326.1320	>99
XIP-des-G1L2D3L7 (P44)	WWS	500.1904(+Na)	500.1883	>99
XIP-des-G1L2D3W4L7 (P45)	WS	314.1111(+Na)	314.1108	>99
XIP-des-G1L2D3S6L7 (P46)	WW	413.1584(+Na)	413.1582	>99

EM = Exact Mass.

Primary reporter gene assay data

Initial agonism screening against *S. mutans* SMCOM2 (*Pcomx*::*lacZ*)

Agonism assays were performed at 100 µM concentration. XIP was used as the positive control (100%) with DMSO as the negative control (0%). Percent (%) ComX activation was measured by normalizing the Miller units obtained for each peptide to that of XIP. All peptides were screened in triplicates over three separate trials. Error bars indicate standard error of the mean of nine values.

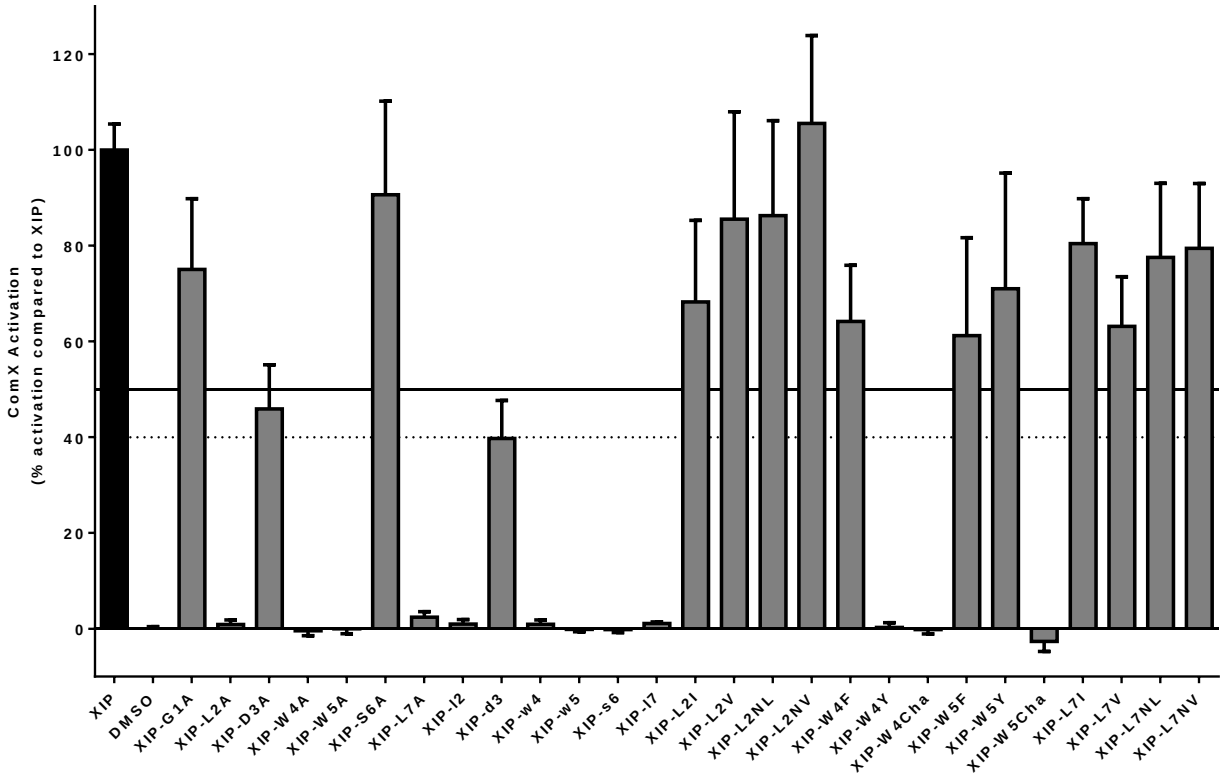

Figure S-1. Primary agonism screening assay data for the XIP analogs. Peptides that exhibited over 50% activation were further evaluated to determine their EC_{50} while peptides that exhibited less than 40% activation were evaluated as potential competitive inhibitors.

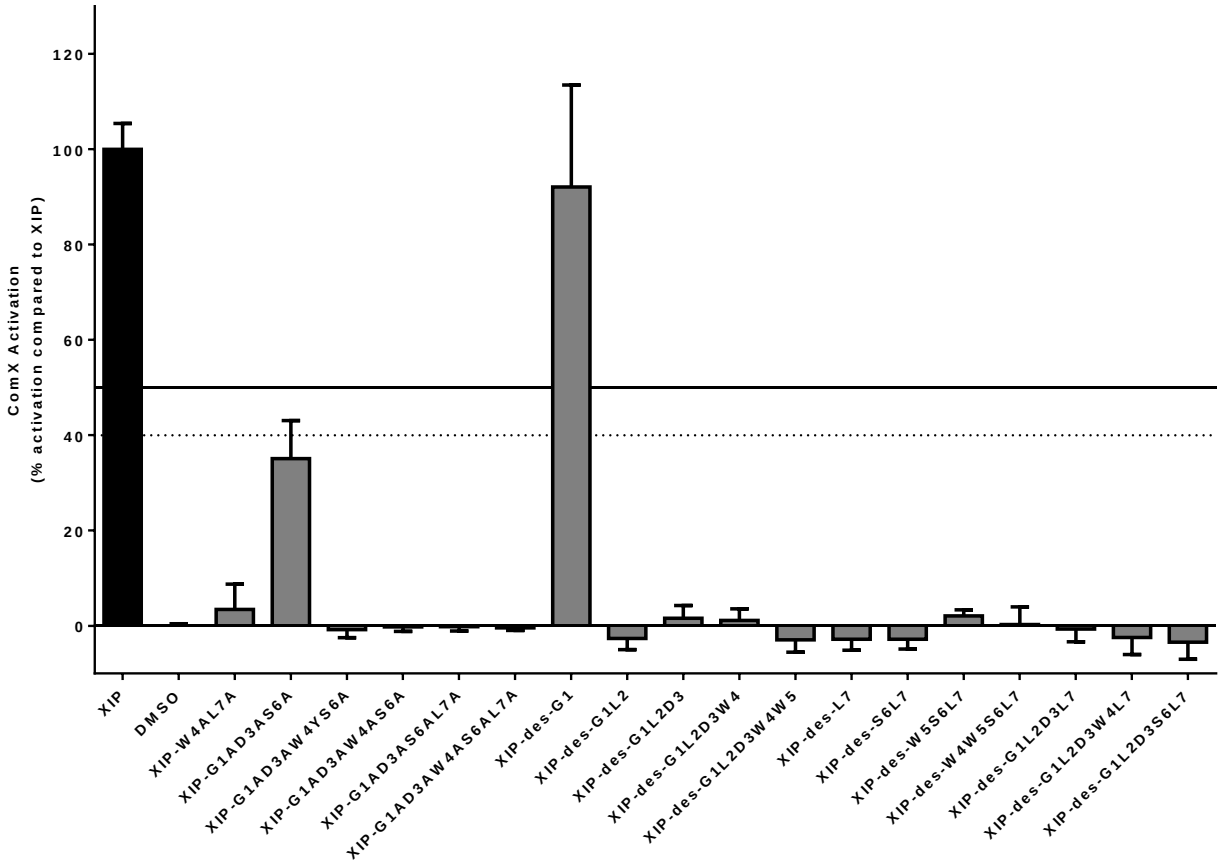

Figure S-2. Primary agonism screening assay data for the XIP analogs. Peptides that exhibited over 50% activation were further evaluated to determine their EC_{50} while peptides that exhibited less than 40% activation were evaluated as potential competitive inhibitors.

Initial antagonism screening against *S. mutans* SMCOM2 (*Pcomx*::*lacZ*)

Antagonism assays were performed at 100 µM concentration of peptides against 2 µM concentration of XIP. XIP (2 µM) was used as the positive control (100%) with DMSO as the negative control (0%). Percent (%) ComX activation was measured by normalizing the Miller units obtained for each peptide to that of XIP. All peptides were screened in triplicates over three separate trials. Error bars indicate standard error of the mean of nine values.

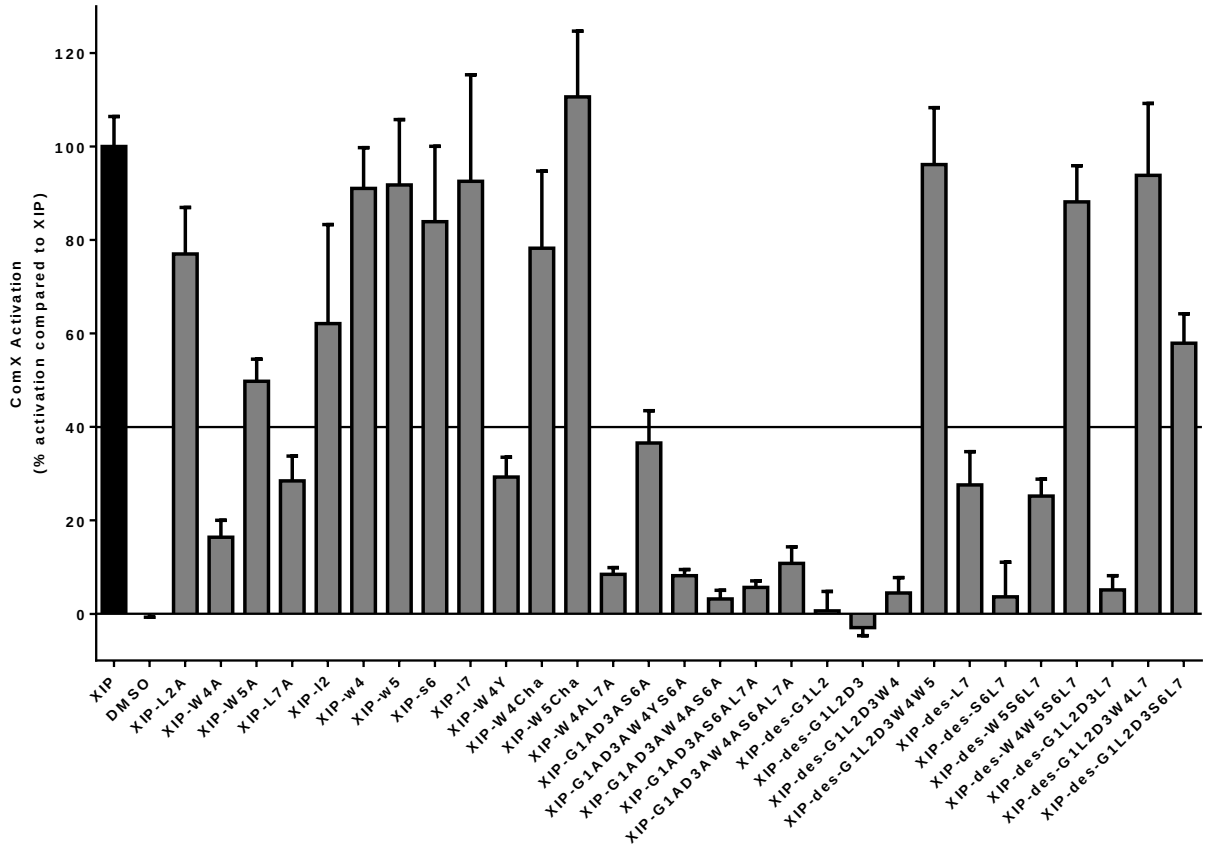

Figure S-3. Primary antagonism screening assay data for the XIP analogs. Peptides that exhibited less than 40% activation were further evaluated to determine their IC_{50}.

Agonism and antagonism dose response curves (SMCOM2 *PcomX::lacZ*)

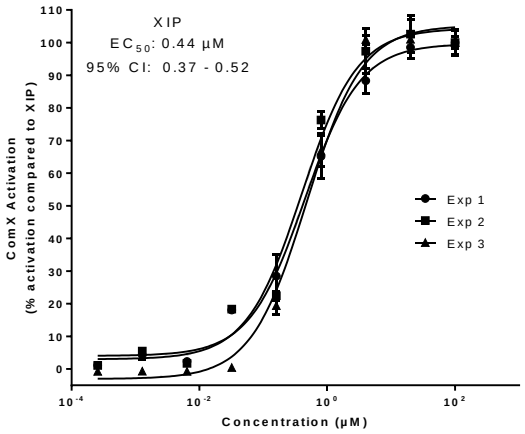

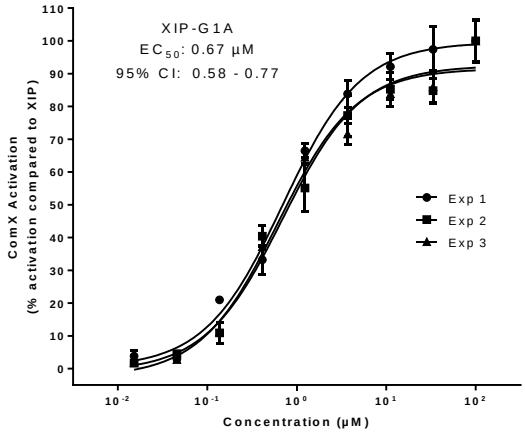

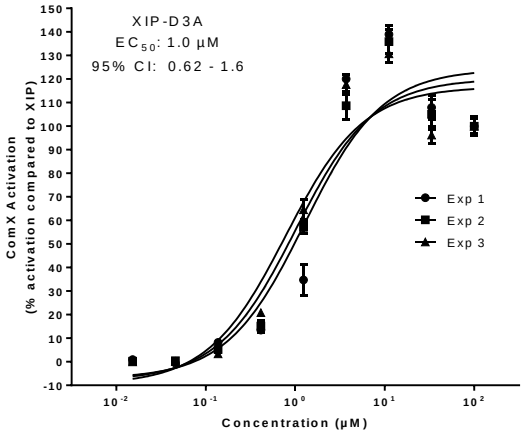

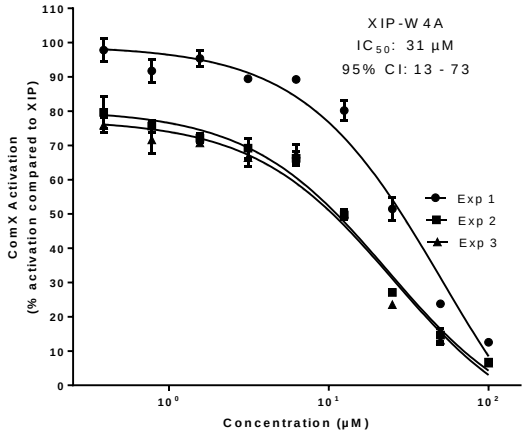

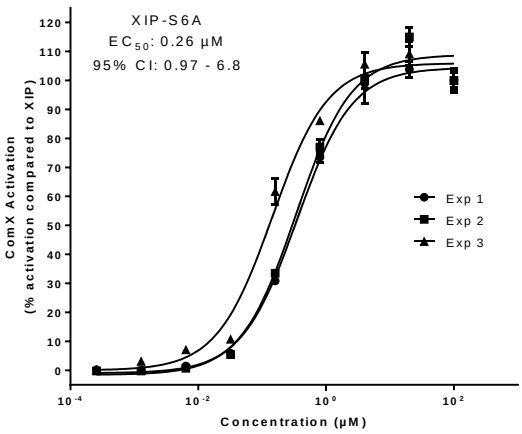

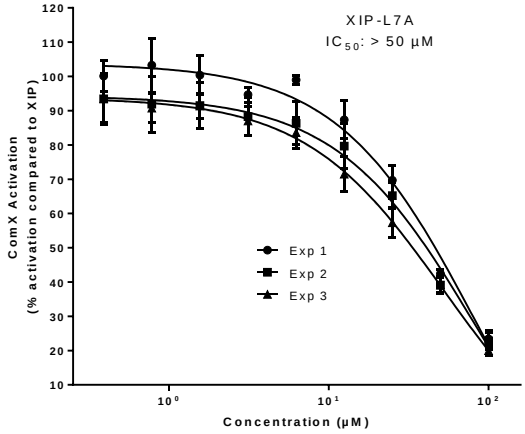

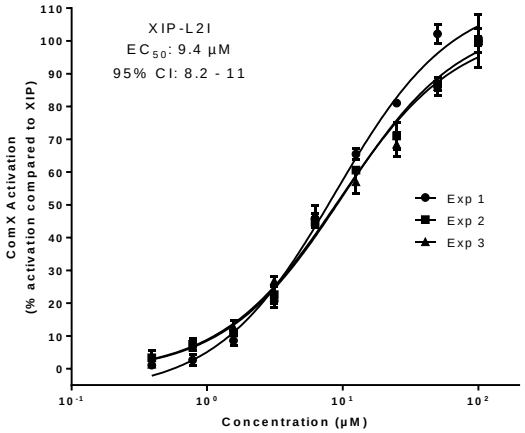
XIP-L2I
EC50: 9.4 µM
95% CI: 8.2 - 11
ComX Activation
(% activation compared to XIP)
Concentration (µM)
Exp 1
Exp 2
Exp 3

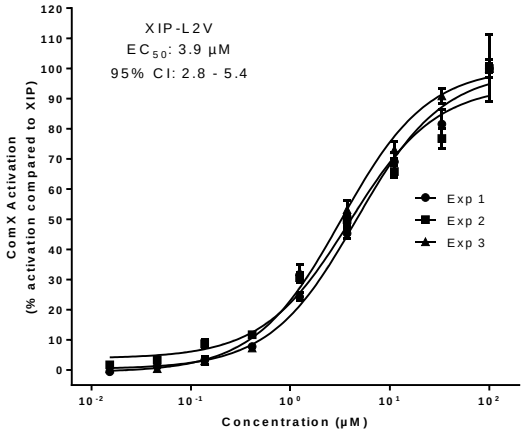
XIP-L2V
EC50: 3.9 µM
95% CI: 2.8 - 5.4
ComX Activation
(% activation compared to XIP)
Concentration (µM)
Exp 1
Exp 2
Exp 3

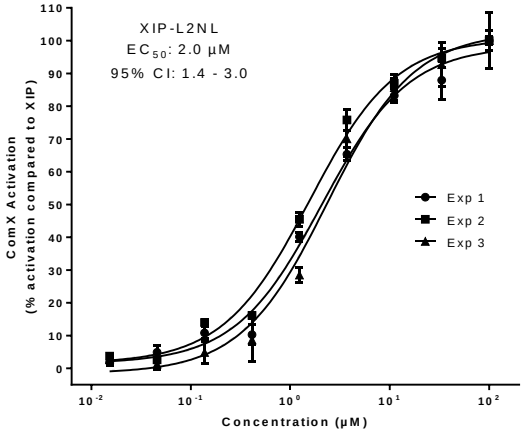
XIP-L2NL
EC50: 2.0 µM
95% CI: 1.4 - 3.0
ComX Activation
(% activation compared to XIP)
Concentration (µM)
Exp 1
Exp 2
Exp 3

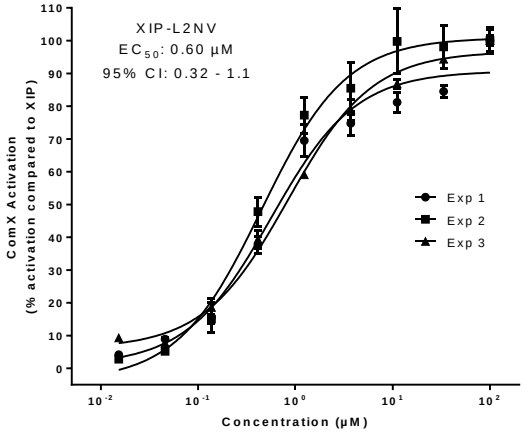
XIP-L2NV
EC50: 0.60 µM
95% CI: 0.32 - 1.1
ComX Activation
(% activation compared to XIP)
Concentration (µM)
Exp 1
Exp 2
Exp 3

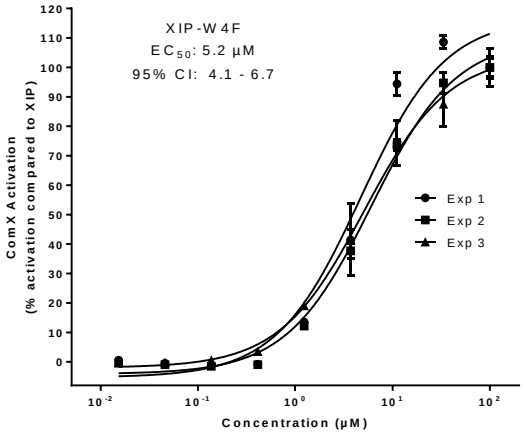
XIP-W4F
EC50: 5.2 µM
95% CI: 4.1 - 6.7
ComX Activation
(% activation compared to XIP)
Concentration (µM)
Exp 1
Exp 2
Exp 3

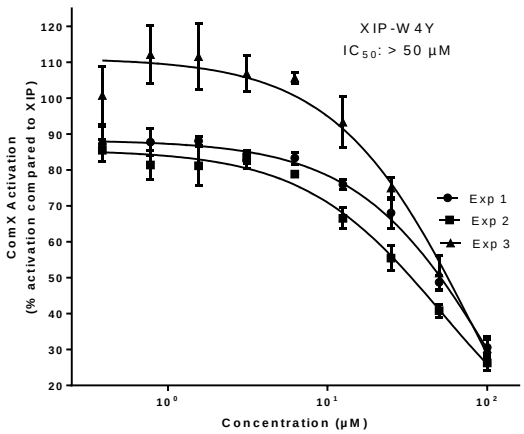
XIP-W4Y
IC50: > 50 µM
ComX Activation
(% activation compared to XIP)
Concentration (µM)
Exp 1
Exp 2
Exp 3

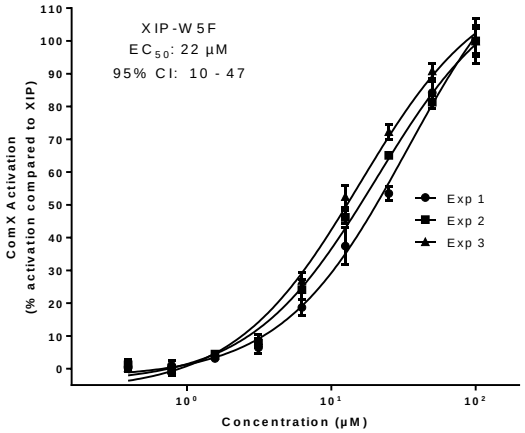
XIP-W5F
EC50: 22 µM
95% CI: 10 - 47
ComX Activation
(% activation compared to XIP)
Concentration (µM)
Exp 1
Exp 2
Exp 3

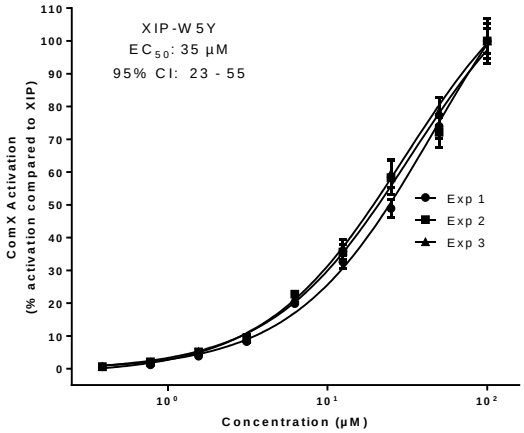
XIP-W5Y
EC50: 35 µM
95% CI: 23 - 55
ComX Activation
(% activation compared to XIP)
Concentration (µM)
Exp 1
Exp 2
Exp 3

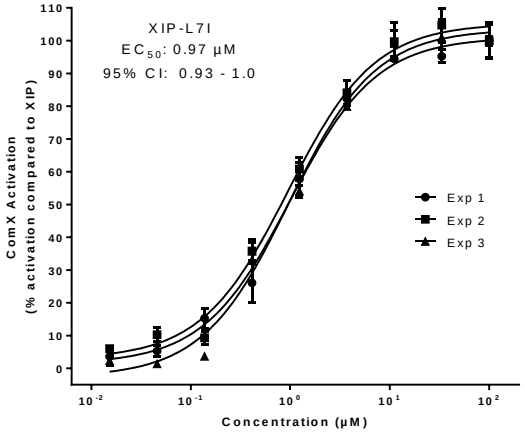
XIP-L7I
EC50: 0.97 µM
95% CI: 0.93 - 1.0
ComX Activation
(% activation compared to XIP)
Concentration (µM)
Exp 1
Exp 2
Exp 3

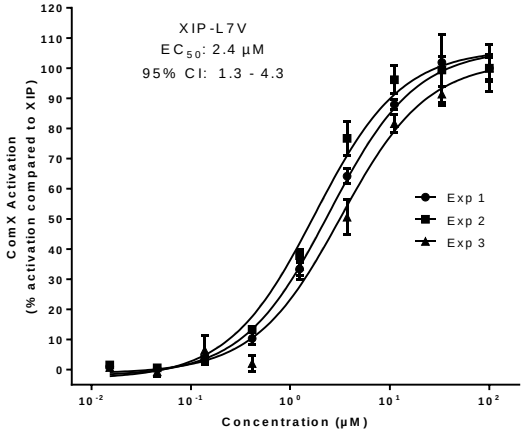
XIP-L7V
EC50: 2.4 µM
95% CI: 1.3 - 4.3
ComX Activation
(% activation compared to XIP)
Concentration (µM)
Exp 1
Exp 2
Exp 3

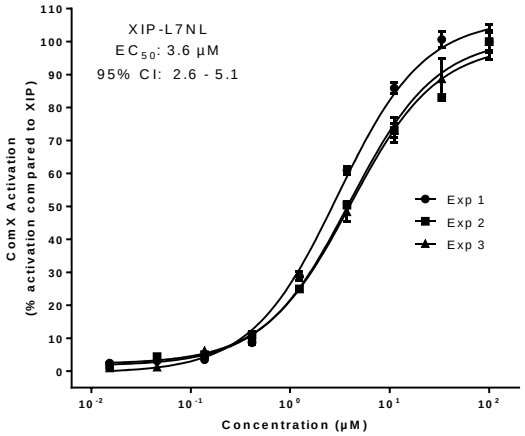
XIP-L7NL
EC50: 3.6 µM
95% CI: 2.6 - 5.1
ComX Activation
(% activation compared to XIP)
Concentration (µM)
Exp 1
Exp 2
Exp 3

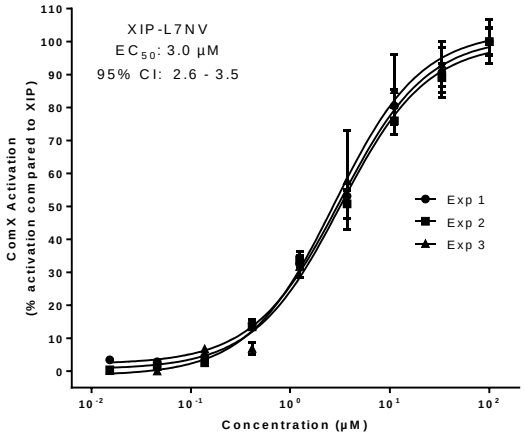
XIP-L7NV
EC50: 3.0 µM
95% CI: 2.6 - 3.5
ComX Activation
(% activation compared to XIP)
Concentration (µM)
Exp 1
Exp 2
Exp 3

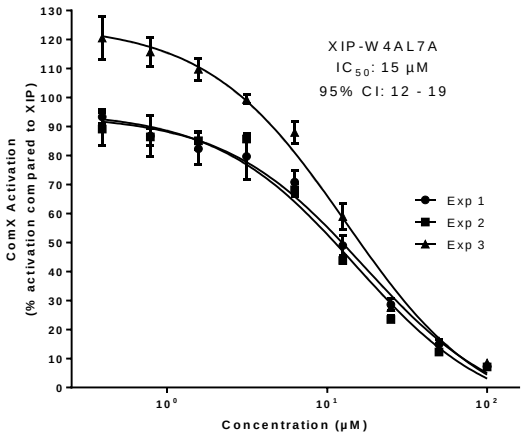
XIP-W4AL7A
IC50: 15 µM
95% CI: 12 - 19
Exp 1
Exp 2
Exp 3
ComX Activation
(% activation compared to XIP)
Concentration (µM)

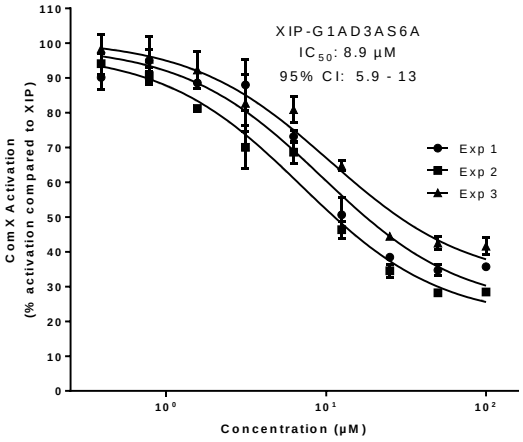
XIP-G1AD3AS6A
IC50: 8.9 µM
95% CI: 5.9 - 13
Exp 1
Exp 2
Exp 3
ComX Activation
(% activation compared to XIP)
Concentration (µM)

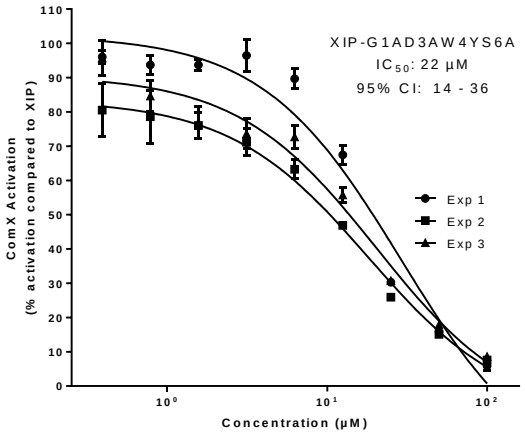
XIP-G1AD3AW4YS6A
IC50: 22 µM
95% CI: 14 - 36
Exp 1
Exp 2
Exp 3
ComX Activation
(% activation compared to XIP)
Concentration (µM)

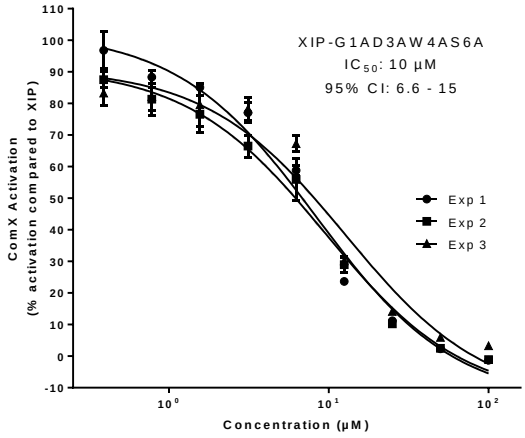
XIP-G1AD3AW4AS6A
IC50: 10 µM
95% CI: 6.6 - 15
Exp 1
Exp 2
Exp 3
ComX Activation
(% activation compared to XIP)
Concentration (µM)

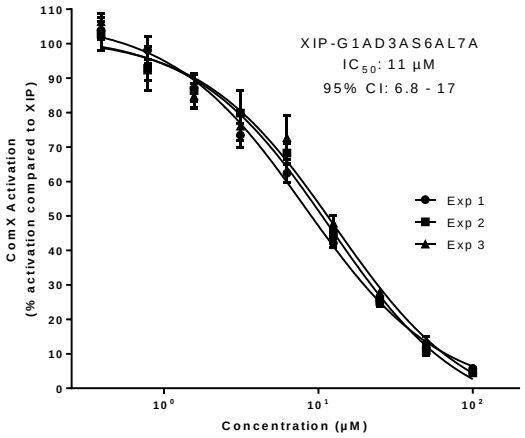
XIP-G1AD3AS6AL7A
IC50: 11 µM
95% CI: 6.8 - 17
Exp 1
Exp 2
Exp 3
ComX Activation
(% activation compared to XIP)
Concentration (µM)

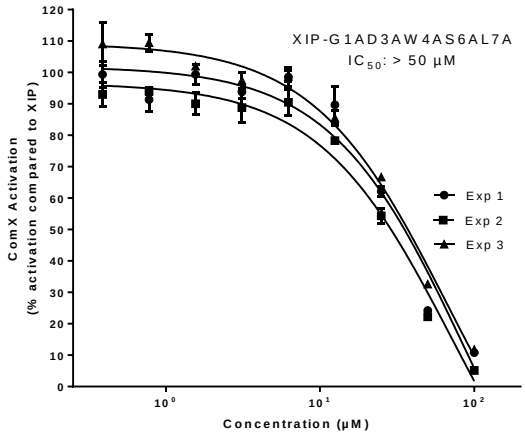
XIP-G1AD3AW4AS6AL7A
IC50: > 50 µM
Exp 1
Exp 2
Exp 3
ComX Activation
(% activation compared to XIP)
Concentration (µM)

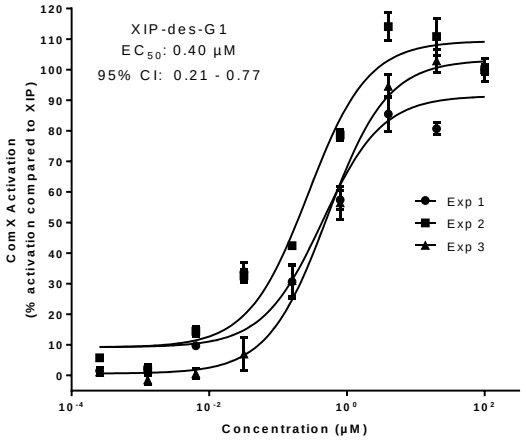
XIP-des-G1
EC50: 0.40 µM
95% CI: 0.21 - 0.77
ComX Activation
(% activation compared to XIP)
Concentration (µM)
Exp 1
Exp 2
Exp 3

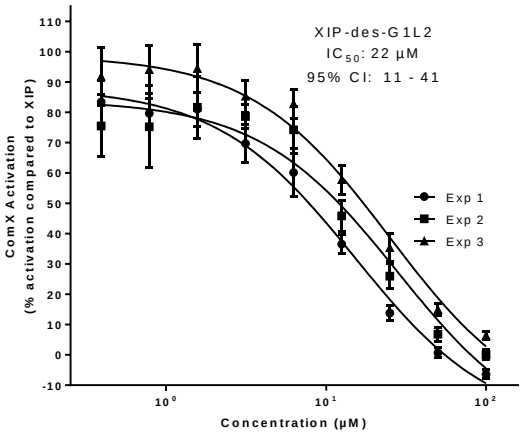
XIP-des-G1L2
IC50: 22 µM
95% CI: 11 - 41
ComX Activation
(% activation compared to XIP)
Concentration (µM)
Exp 1
Exp 2
Exp 3

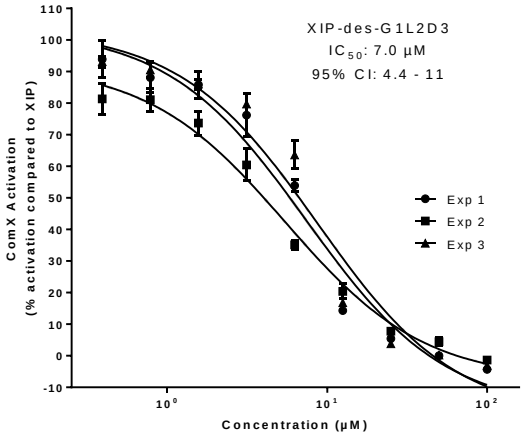
XIP-des-G1L2D3
IC50: 7.0 µM
95% CI: 4.4 - 11
ComX Activation
(% activation compared to XIP)
Concentration (µM)
Exp 1
Exp 2
Exp 3

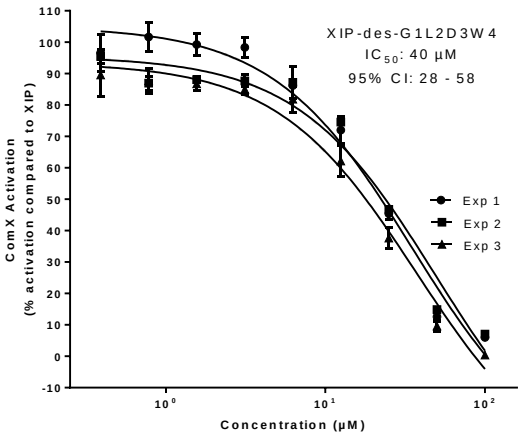
XIP-des-G1L2D3W4
IC50: 40 µM
95% CI: 28 - 58
ComX Activation
(% activation compared to XIP)
Concentration (µM)
Exp 1
Exp 2
Exp 3

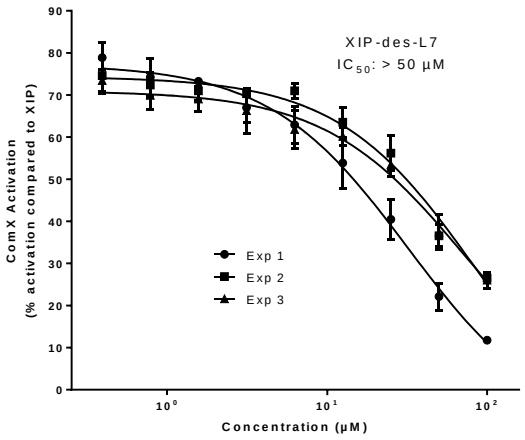
XIP-des-L7
IC50: > 50 µM
ComX Activation
(% activation compared to XIP)
Concentration (µM)
Exp 1
Exp 2
Exp 3

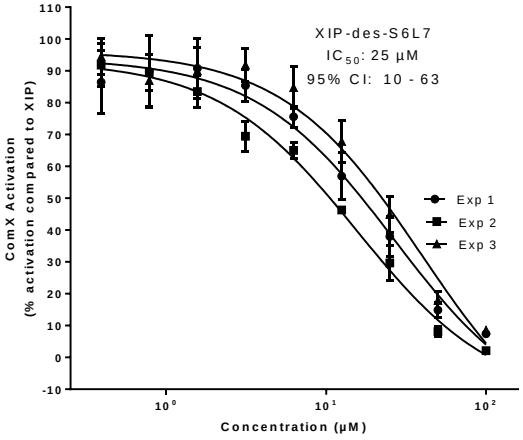
XIP-des-S6L7
IC50: 25 µM
95% CI: 10 - 63
ComX Activation
(% activation compared to XIP)
Concentration (µM)
Exp 1
Exp 2
Exp 3

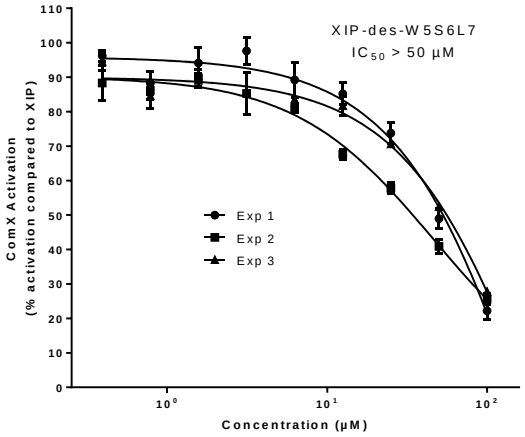
XIP-des-W5S6L7
IC50 > 50 µM
ComX Activation
(% activation compared to XIP)
Exp 1
Exp 2
Exp 3
Concentration (µM)

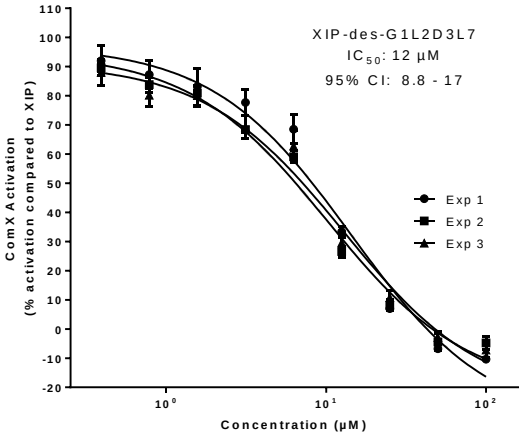
XIP-des-G1L2D3L7
IC50: 12 µM
95% CI: 8.8 - 17
ComX Activation
(% activation compared to XIP)
Exp 1
Exp 2
Exp 3
Concentration (µM)

Crystal violet biofilm formation assay

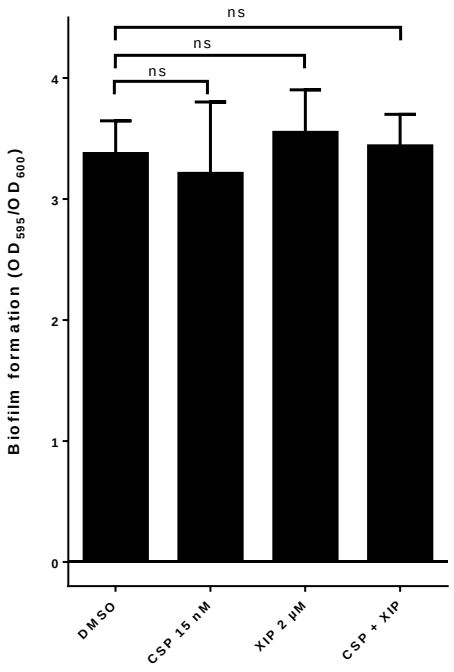

Figure S-4. Biofilm formation of *S. mutans* UA159 (wildtype) in the presence of 18-CSP (15 nM), XIP (2 µM), CSP + XIP, or DMSO (negative control). No significant changes were observed in the presence of either CSP or XIP or both (CSP and XIP). ns, non-significant.

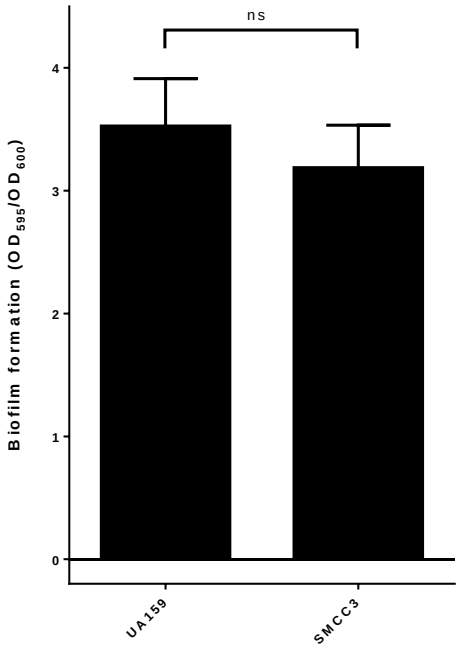

Figure S-5. Biofilm formation of *S. mutans* UA159 (wildtype) and SMCC3 (Δ*comC* mutant). ns, non-significant.

Interspecies Inhibition assay

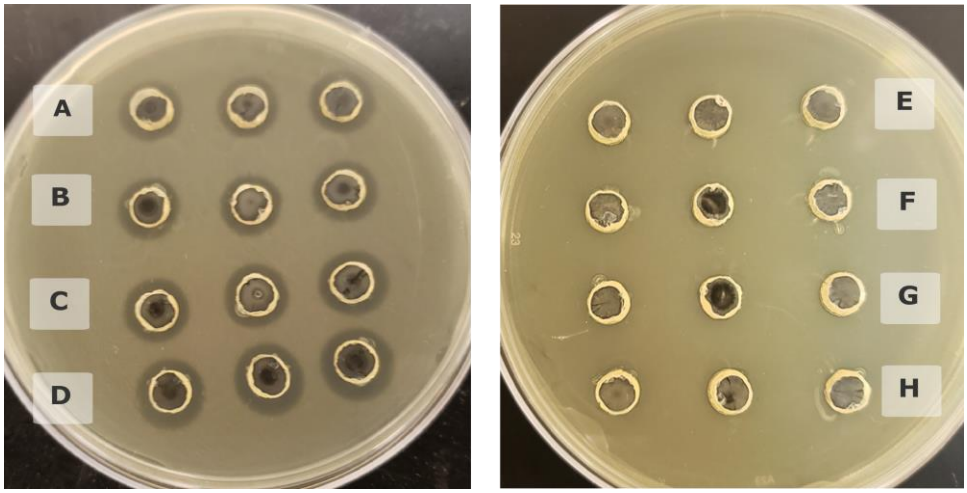

Figure S-6. Interspecies inhibition assay between *S. mutans* and *S. anginosus*. *S. mutans* SMCC3 (Δ*comC*) was tested for its ability to inhibit the growth of *S. anginosus* ATCC 33397 when SMCC3 was treated with (A) 15 nM 18-CSP, (B) 15 nM 18-CSP + 2 µM XIP, (C) 15 nM 18-CSP + 100 µM P32, (D) 15 nM 18-CSP + 2 µM XIP + 100 µM P32, (E) 2 µM XIP, (F) 100 µM P32, (G) 2 µM XIP + 100 µM P32, and (H) DMSO. Each assay was repeated on three separate days.

Lactic acid production assay

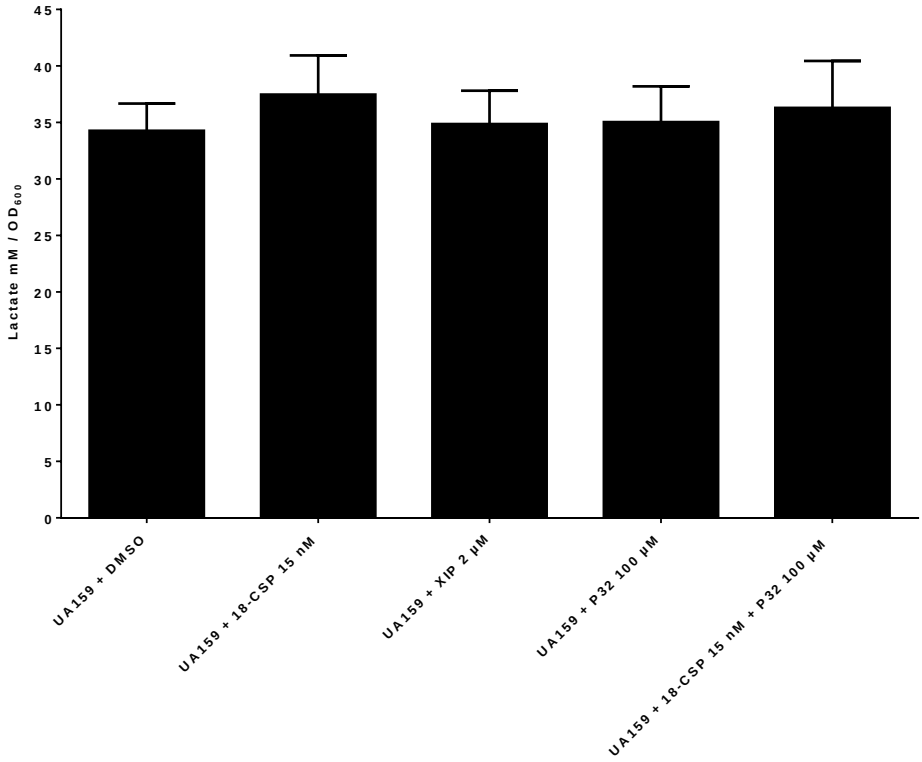

Figure S-7. Lactic acid production assay. *S. mutans* UA159 was treated with either DMSO (control), 18-CSP, XIP, P32, or 18-CSP + P32, and lactic acid production was quantified using an EnzyChrome lactate assay. Similar levels of lactic acid were observed for all conditions. The assay was repeated in triplicate on three separate days.